HAWASSA UNIVERSITY

INSTITUTE OF TECHNOLOGY

FACULTY OF ELECTRICAL ENGINEERING

DEPARTMENT OF ELECTRICAL AND COMPUTER ENGINEERING

PERFORMANCE COMPARISON OF CHANNEL MODELS FOR UFMC SYSTEM

By

TILAHUN BELAYNEH MAMO

ADVISOR: DR. KINDE ANLAY

CO-ADVISOR: SAMSON ALEMAYEHU (M.sc)

A THESIS

SUBMITTED TO THE DEPARTMENT OF ELECTRICAL AND COMPUTER ENGINEERING, IN PARTIAL FULFILLMENT OF THE REQUIREMENTS

FOR THE DEGREE OF

MASTER OF SCIENCE

IN

COMMUNICATION ENGINEERING AND NETWORKING STREAM

June 29, 2019

Hawassa,
Ethiopia

ACKNOWLEDGEMENT

This thesis is completed with prayer of many and love of my family and lovely wife **Tagyee.M**. However, there are few people that I would like to specially acknowledge and extend my heartfelt gratitude who have made the completion of this thesis possible. With the biggest contribution to this thesis; I would like to thank my advisor Dr. **Kinde Anlay** had given me his full support in guiding me with stimulating suggestions and encouragement to go ahead in all the time of the thesis. I would also like to thank co-advisor **Mr. Samson Alemayehu** for his kind support during this work. I am also thankful to **Mr. Mesfin Fanuel,** Head, Electrical and Computer Engineering Department, for providing us with the adequate infrastructure in carrying the work. I am also thankful to **Mr. Fishum** Coordinator, Communication stream department, for the motivation and inspiration that triggered me for the thesis.

At last but not the least my gratitude towards my parents, I would also like to thank **GOD** for not letting me down at a time of crisis and showing me the silver lining in the dark clouds.

Table of Contents

LIST OF FIGURE

LIST OF TABLE

LIST OF ABBREVIATION

16-DPSK……..……16-Differential Phase Shift Key

5G ……5 Generation

64-QAM……...64 Quadrature Amplitude Modulation

AWGN…….Additive white Gaussian noise

BD……Doppler spread

BER……..……Bit Error Rate

CDF……..Cumulative Distribution Function

CDMA 2000…….Code Division Multiplexing Access

CP…….Cyclic Prefix

FBMC ……..Filter Bank Multi Carrier

FFT…….…..Fast Fourier Transform

GSM…….....Global System Mobile Communication

IFFT…….....Inverse Fast Fourier Transform

ISI……..Inter Symbol Interference

LTI…….Linear Time Invariant

LTV…….. Linear Time Variant

MGF……..Moment Generating Function

MIMO…….. Multiple- Input Multiple Output

MLSE……Minimum Least Square Error

MMSE…….. Minimum Mean Square Error

NCP…….……Number Cyclic Prefix

NCS.....Number Cyclic Suffix

OFDM …….…….....Orthogonal Frequency Division Multiplexing

OOB…….Out of Band

PAPR…….....Peak To Average Power Ratio

PDF ……..Probability Distribution Function

RB…… Resource Block

Rx…….Receiver

SNR……..Signal to Noise Ratio

Tb……..…Symbol Period

Tc…….....Coherence Time

UFMC……..Universal Filtered Multi-Carrier

Wi-Fi……Wireless Fidelity

ZF…….Zero forcing

ABSTRACT

This paper presents the bit error rate (BER) vs. signal-to-noise (SNR) ratio performance of channel models under UFMC system with 32- FSK, PAM, DPSK, 4-QAM, 16-QAM, 32-QAM, 64-QAM and 128-QAM modulation. In future it is believed to be more challenging and complicated with the evolution of different types of fading model. These types of fading models determined in urban and rural areas. Rayleigh fading model is considered to be most common fading model, found in urban environment for non-line of sight. Rician fading consists of line of sight communication and found to be more applicable for satellite communication. Nakagami fading model is mostly suited for urban multipath propagation and it is sought to be most practical model, specially used in mobile communication. In order to achieve error free signal at the receiver the choice of modulation scheme should be done wisely. The combination of best efficient modulation scheme along with the block coding helps in getting the signal error free at the receiver. The condition of signal is decided by SNR v/s BER (bit error rate) simulation. Our main objective is to get error free result at the receiver, so for this different data transmission techniques are used to transmit the data from transmitter to receiver in various fading channels under different modulation schemes. Effect of shape factor on Nakagami fading is also covered in this thesis to get efficient results. The BER performance was to compared with Additive White Gaussian Noise (AWGN), Rayleigh-faded, Nakagami-m faded and Rician-faded channels. It has been further concluded that the BER vs. SNR performance graph in AWGN channel environment is better than that in Rayleigh, Nakagami-m and Rician-faded channel. It is also observed that by varying the standard-deviation of the channel, the BER vs. SNR performance graph is not going to be affected if the channel is considered Rayleigh-faded. In this paper we address a new aspect of UFMC system performance by investigating its capability to overcome the channel fading channels' effects and to provide good and reliable performance levels overcome these channel effects.

Key word: UFMC, Rayleigh, Rician, Nakagami, AWGN, capacity

Chapter One: Introduction

1.1. Background

The fifth generation it was various modulation techniques are used in under different communication system such as orthogonal frequency-division multiplexing (OFDM), universal filtered multicarrier (UFMC), filter bank based multi-carrier (FBMC generalized frequency division multiplexing (GFDM) and etc. The orthogonal frequency-division multiplexing (OFDM) and its different schemes orthogonal frequency division multiple access (OFDMA) in the long-term evolution (LTE) system) are widely applied for wireless and underwater communications [1].

The advantages of OFDM are the capability to support the usage of the adjustable channel bandwidth, lower signal processing complexity, seamless integration with Multi-input Multi-output (MIMO) systems, ability to accomplish users scheduling both in time and frequency domain and its inherent robustness to combat multipath effect. Although it has efficient implementation and robustness to channel delays as highlights but this method suffers from high PAPR results low efficiency of power amplifier, increases the battery consumption. Moreover the OFDM spectrum has high out of band side lobes causing problem of low spectral efficiency. To overcome some of these drawbacks new modulation techniques for 5G communication system are considered. The applications which use 5G communication system require higher data rates, lower latency and efficient spectrum usage. The way to overcome the known limitations of OFDM is UFMC technique. UFMC is generalization of Filtered OFDM and FBMC modulations [2].

The filter bank multi-carrier (FBMC) has triggered much attention as a replacement for OFDM in recent times. The FBMC scheme utilizes an integrated poly-phase filter-bank to offer a very strong side lobe suppression function by filtering each subcarrier. However, in FBMC, each subcarrier is filtered separately by the means of dedicated filter, hence, results in increasing computational burden when compared to its filtered version, i.e., filtered-OFDM or the traditional OFDM scheme [3].

The universal filtered multicarrier (UFMC) has been proposed to solve to reduce peak to average power ratio (PAPR), out of band (OOB), reduce the latency, complexity and reduce

battery consuming. The subcarriers are grouped in subsets are subject to be filtered in the UFMC transmitter, therefore, not only reduce the required number of filters, but also simplify the transceiver configuration. The UFMC scheme can be treated as a mid-solution between the FBMC method and filtered OFDM technique in terms of computational complexity. The UFMC usages one-tap channel equalization technique with low-complexity, provides much lower OOB emission than filtered OFDM and FBMC, channel estimation and equalization algorithms with low-complexity and ease in the implementation with MIMO systems without generating significant inter service band interference. The aforementioned advantages make the UFMC as one of the most potential candidate waveforms for 5G systems and beyond [4].

In OFDM the total band is filtered and in Filter Bank Multi-Carrier (FBMC) individual subcarriers are filtered where as a group of subcarriers (sub bands) are filtered in UFMC. This subcarrier grouping reduces the filter length (when compared with FBMC). Single carrier modulation uses one carrier to transmit overall data. This technique is widely used in GSM, CDMA 2000. The main goals to favor this method are battery power and coverage extensions. Single carrier method requires equalizers to get high spectral efficiency [1-3]. Multicarrier modulation converts a wideband carrier into multiple orthogonal narrowband carriers. For higher data transmission wireless communication systems required to integrate Multicarrier modulation

UFMC waveform is a derivative of OFDM waveform combined with post-filtering, where a group of carriers is filtered by b using frequency domain efficient implementation [1-3]. The filtering operation leads to a lower out-of-band leakage than for OFDM. The UFMC transmitter is composed of sub-band filtering that modulate the data blocks. The transmitted signal uses no CP, but there is still a spectral efficiency loss due to the time transient (tails) of the shaping filter. The new waveform should achieve the asynchronous reception and transmission, non-orthogonal waveforms for better spectral efficiency and low latency. But at the same time, you can easily tune the subcarriers spacing and number of tones depending upon the band range and bandwidth of application that we are dealing with. In addressing scalable waveform on the same network, we can introduce filtering to the OFDM symbols that we can actually have different numerology coexistence on the same network. Some new waveform designs are more attracted by industries as well as research organizations which are less complex in design, UFMC is the most adequate for 5G [5].

UFMC is the method that combines the advantages of orthogonality OFDM and filter bank in FBMC. Instead of filtering each carrier like in FBMC, we have to filter a block of carriers called sub-band. Each sub-band contains a number of carriers; filter length will be depending upon the width of sub-band. In the UFMC system, the complex symbols generated from the base - band modulator. These complex symbols are converted to parallel stream, make a block of streams and given as input to the IFFT of their respective. The length of N point IFFT output will be serialized as block-wise and that output will be filtered with a pulse shaping filter of length L [6].

1.2. Statement of the Problem

The main challenges in modern wireless communication systems are signal fading. UFMC wireless channel was random in nature, so the signal are received from transmitter by multipath i.e. reflection, diffraction and scattering in addition to direct line of sight path. These conditions can occur due to the mobility of the receiver or the size of communication environment. In UFMC wireless communications, signals that reach the receiver by more than one path are known as a multipath propagating signal. When you compared UFMC, FBMC and OFDM communication systems, OFDM has to face many challenges when consider for adoption in more complex networks. For instance, the use of OFDM in the uplink of the multi user networks known as Orthogonal Frequency Division Multiple Accesses (OFDMA) requires full synchronization of the user's signals at the base station input. Such synchronization was found to be very difficult to establish especially in mobile environments where Doppler shifts of different users are hard to predict, which leads to inter carrier interference (ICI). Further since filters associated with OFDM carrier which have relatively large sidebands. This results in Out Of Band (OOB) radiations. Insufficient spectral usage provided by CP-OFDM by using more guard band. The challenges caused by conventional OFDM/CP-OFDM can be overcome by employing new system termed as Filter Bank Multi Carrier System (FBMC). Instead of filtering the whole band as in the case of OFDM, FBMC filters each sub carrier individually. UFMC is a generalization of filtered OFDM and FBMC modulations. The main objective of this paper is to compare the performance of channel models under UFMC modulation techniques waveform for 5G communication in terms of BER vs SNR with in various modulation schemes.

1.3. Objective

1.3.1. General objective

The main objective of this thesis is the performance comparison of UFMC under Rayleigh, Rician Nakagami-m and AWGN Channel Models

1.3.2. Specific objective

- ✓ To analysis the channel models with various modulation schemes.
- ✓ Analysis the capacity of UFMC system for Rician, Rayleigh, Nakagami-m and AWGN channel models
- ✓ Compare the performance of UFMC system for Rician, Rayleigh, Nakagami-m and AWGN channel models with in different modulation schemes.

1.4. Literature Review

July 2011,in the author, A. Sudhir BabuAssociate Professor [7] In this paper, The Bit Error Ratio of a digital communication system is an important figure of merit used to quantify the integrity of data transmitted through the system. By implementing the different modulation techniques, the criterion is comparison of the variation of BER for different SNR. It is observed that the BER is minimum for AWGN and maximum for RAYLEIGH and RICIAN. For RICIAN it is found that the BER is less than AWGN and RAYLEIGH except in case of 16-DPSK. And it is observed that 16-QAM is performing better than 64-QAM. For higher values of Eb / N0, the BER is decreasing in all the fading channels for different modulation schemes.

May 2011,**in the author**,**Pallavi Bhatnagar, Jaikaran Singh, Mukesh Tiwari [8]**, . In this paper performance of MIMO OFDM is characterized with low complexity. The Rayleigh distribution assumes that there are a sufficiently large number of equal power multipath components with different and independent phase. On basis of the simulated results, it was concluded that the structure has low bit error rate when MLSE equalizer is used. It is shown through numerical simulations that high performance gain is achieved in equalized MIMO OFDM system. The gap of this thesis is used only Rayleigh channel models that not used other alternative models like AWGN, Nakagami-m and etc.

Suchita Varade, Kishore Kulat [9] "In this paper performance comparison of chaotic communication based MIMO-OFDM system is given with and without using adaptive beamforming. The use of chaotic communication system can increase the security prospective of the system due to it bifurcation behavior when varying the initial condition. The proposed scheme has been verified in AWGN channel, Rayleigh Fading channel and Rician Fading channel. It has been observed that BER performance of the system is improved with adaptive beamforming. Channels perform in the following order in terms of best (less SNR requirement) to worst (more SNR requirement) to maintain the required BER: AWGN, Rician, Rayleigh. The gap of this thesis is depend on channel models only there is no analysis on various types mapping schemes with in cognitive radio.

A. Sudhir Babu, Dr. K.V Sambasiva Rao [10] In this paper, we evaluated the performance of available transmission modes in IEEE 802.11b. The performance of transmission modes are evaluated by calculating the probability of Bit Error Rate (BER) versus the Signal Noise Ratio (SNR) under the frequently used three wireless channel models (AWGN, Rayleigh and Rician). From the simulation results, the Bit Error Ratio of a digital communication system is an important figure of merit used to quantify the integrity of data transmitted through the system. By implementing the different modulation techniques, the criterion is comparison of the variation of BER for different SNR. It is observed that the BER is minimum for AWGN and maximum for RAYLEIGH and RICIAN. For RICIAN it is found that the BER is less than AWGN and RAYLEIGH except in case of 16- DPSK. And it is observed that 16-QAM is performing better than 64-QAM. For higher values of Eb / N0, the BER is decreasing in all the fading channels for different modulation schemes. The performance evaluation nice nothing but how about the outage probability that means the probability distribution function (PDF) and cumulative distribution function (CDF). In addition to this we done on PDF and also add Nakagami-m channel model.

July-August-2015, **Yashraj Singh1, Mrs. Anita Chopra2 [11].**

In this paper demonstrate the comparison of the Rayleigh, Rician and Nakagami fading channel models by using MATLAB simulation in terms of source velocity and probability density function. We have developed algorithms for above channel, which calculate the Reference signal, inphase signal, Quadrature Signal, Envelope Signal, Probability density function.

Major objective of this work (for which this research has been carried out) has the major outcome that the probability density function of Nakagami-m is fading channel increases with respect to Rayleigh and Rician fading channel. In Nakagami-m fading channel has sum of multiple independent and identically distributed Rayleigh-fading signals have Nakagami distributed signal amplitude. The Nakagami-m is generalized channel model which can be converted to Rician distribution, Rayleigh distribution. This paper gap was not depend on SNR vs BER. This paper performance analysis of Rayleigh Rician Nakagami-m and AWGN channel models with in SNR and BER for UFMC system.

In,the authors, Shravan Kumar Bandari and V.V. Mani [12]. The purpose of this paper is to study the performance of generalized frequency division multiplexing (GFDM) in some

frequency selective fading channels. The exact symbol error rate (SER) expressions in Hoyt (Nakagami-q) and Weibull-v fading channels are derived. A GFDM transceiver simulation test bed is provided to validate the obtained analytical expressions. In summary, for Hoyt-q fading and fixed pulse shaping filter parameter α, we observed a significant SER decrease as the Hoyt fading parameter q increased from the value 0.2 to 1. Similarly, as the Weibull fading parameter υ is increased, there is a significant decrease in the SER for a fixed value of α. This implies that GFDM exhibits better error performance for strong fading conditions than conventional OFDM.
In this thesis the performance comparison of Rician, Rayleigh, Nakagami-m channel fading and AWGN channel for UFMC system and also to identify the appropriate channel model from those in terms of BER verses SNR and also additionally Capacity verses SNR.

1.5. Methodology

Generally, the methodology mainly consists of the following parts:

- First, reviews of different research papers which are closely related to this thesis
- After reviewing those literatures done so far by other scholars, we theoretically give explanation regarding the UFMC system.
- Then, Rayleigh, Rician, Nakagami-m and AWGN models under UFMC system for their detailed block diagram and description of each block. Particularly when the data was transmitted by the transmitter, channel fading and noise was added to the signal. At the receiver, the same signal was detected, dividing it by the same channel response that was added to it. Numbers of errors are calculated by comparing the transmitted and the received data. Signal and Noise power are calculated which then help in calculating the signal to noise ratio for the system.
- Plot the comparison of the channel fading's using MATLAB software tool.
- Finally, analysis performance and capacity for the channel models under UFMC system simulation result with brief description.

1.6. Scope of Thesis

Performance analysis of different types of channel fading for UFMC system in terms of several parameters is possible but, this thesis performs the capacity analysis of the UFMC system using Rayleigh, Rician AWGN and Nakagami fading its BER vs. SNR, outage probability of PDF

1.7. Outline of the Thesis

The thesis is structured as follows:

Chapter 2 deals with the UFMC and also channel model used in the thesis. It discusses the basic concepts and assumptions required to formulate a suitable channel model.

Chapter 3 discusses the characterization and application of probability distributions which are relevant to model fading channels. Furthermore, the different statistical fading channel models are described in detail with in formula.

Chapter 4 analyzes and discusses channel performance measures for fading channels in the under UFMC. The key performance measures which are considered in the analysis are average BER vs. SNR, outage probability, and average capacity.

Chapter 5 concludes the thesis work by pointing out its accomplishments and recommends further extensions for the research.

Chapter Two: System Design

2.1. UFMC System Design

Now-a-days UFMC is a highly research involved 5G modulation method. UFMC, a new multicarrier modulation technique works equivalent to the generality of filtered OFDM and FBMC modulations. Unlike self-subcarrier modulation in FBMC, a group of subcarrier modulation is performed in UFMC. The subcarrier grouping reduces the length of the filter compared with FBMC and also reduces time to perform modulation [13].

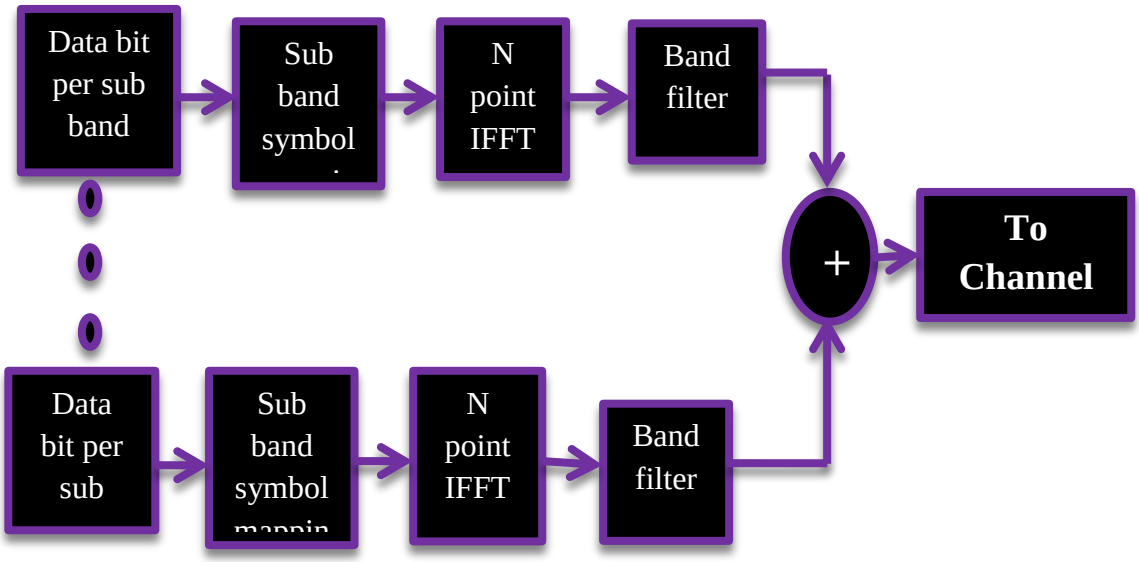

Figure 2.1 UFMC transmitter block diagram [14]

UFMC employs the division of full band into sub bands. The modulation technique processes these sub bands individually and each sub band consists of fixed number of subcarriers. The narrowband and closely spaced Individual sub bands undergoes N-point Inverse Fast Fourier Transform (IFFT) to get time domain of each sub band from Frequency Domain of each sub band. Each sub band output resulting from IFFT is filtered by filter length L. The resulting output signal is expressed as IFFT operation ensures that the sub band carriers do not interfere. UFMC uses Band filter to perform a Chebyshev filtering operation. Band Filter filters each sub band and each sub band responses summed. The filtering approach in UFMC reduces out of band spectral emission for proper design of filter. Filter with parameterized side lobe attenuation is employed to filter the IFFT output per sub band. UFMC receiver performs 2N point Fast Fourier Transform (FFT) on data obtained from channel.

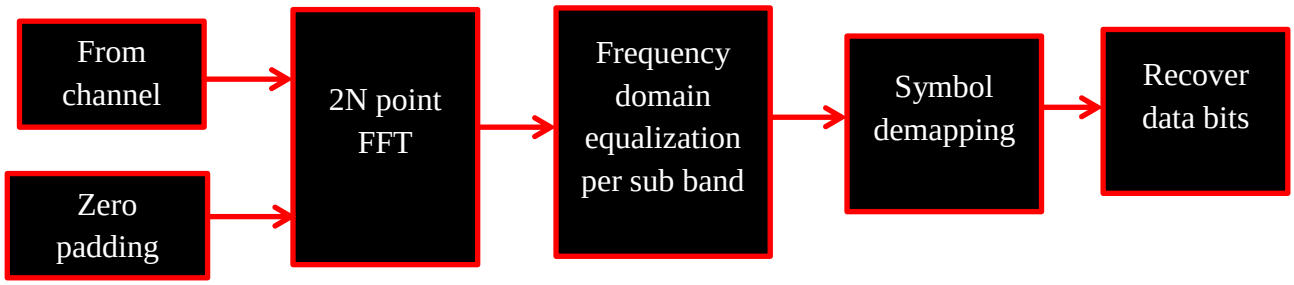

Figure 2.2 UFMC receiver block diagram [14]

A guard interval of Zeros is added between successive IFFT symbols. This prevents the Inter Symbol Interference (ISI) due Transmitter filter delay. Discard even subcarrier points to get N length frequency domain receive signal. FFT coverts data received in time domain into frequency domain. Equalization detects the transmitted data. The Symbol demapping is performed prior to the frequency domain equalization to get the original data bits.

2.2. Communication System Model

Figure 2.3 shows the block diagram of a conceptual communication system that is usually employed in the mathematical analysis of information transmission. The model is introduced by C. E. Shannon, the father of information theory, in the mid-20th century. It comprises blocks denoting information source and destination, designed transmitter and receiver, and transmission channel. The information required to be transmitted successfully to the information sink is generated at the information source. The transmitter and the receiver are digital signal processors that are designed for a successful transmission. The behavior of the transmission medium that cannot be influenced by the system engineer is depicted by the channel block, residing at the center of the model diagram. The design of a successful communication system requires a good model for the transmission channel. In other words, having a good description of the communication channel enables better design of the system.

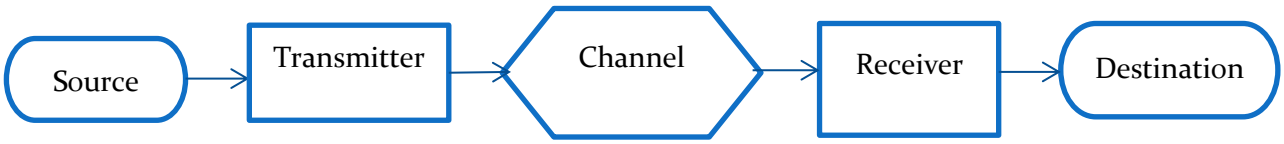

Figure 2.3 Communication system model [15]

So far, experts have worked hard to describe phenomena accompanying different channels, and at the same time to come up with some descriptive and simple mathematical models for further

analysis of the system. Actually, there are three channel models that are commonly used in the analysis of a communication system. These models are Additive White Gaussian Noise (AWGN), Linear Time Invariant (LTI) and Linear Time Variant (LTV) channels. AWGN channel is the simplest channel model that considers only single channel impairment: noise $c(t)$.The model is it does not take into account the effect of any fading or distortions. This model is usually used to come up with controllable mathematical models of communication system functionalities so that a better understanding of a system without fading and other distortions is possible. Furthermore, this model is well suited for wired and satellite communication.

The second model, LTI channel model, includes deterministic linear distortion in addition to the random AWGN. Here, the deterministic distortion is modeled by a linear time invariant filter with an impulse response of $c(t)$.This model is usually applied to analyze and design the functionalities of both transmitter and receiver since linearity and time invariability properties of the filter enables usage of good mathematical tools. Most wireless channels are time variant due to the mobility of the transmitter and receiver and hence the third model called as LTV channel is used. In this model, time varying filter with impulse response $h(\tau, t)$ is used. Here $h(\tau, t)$ is the response of the channel at time t due to an impulse applied at time $t - \tau$. This model is more complex than LTI channel. As a result, LTI channel model may still be used given that the channel is varying slowly compared to the time scale of the communication processes analyzed [16].

2.3. Channel Model

Modeling the terrestrial wireless propagation was the importance for the design and performance analysis of wireless communication systems. Unlike wired propagation situations which are motionless and expectable in a typical mobile radio propagation condition, the received signal presents both small-scale power fluctuations also known as multipath fading and large-scale power fluctuations also known as shadowing. In the former, the transmitted signal experiences reflection, diffraction, scattering, and delays, whereby the multipath phenomenon was caused by a relatively fast constructive and destructive random combination of the received signal duplicates. Large-scale signal power fluctuations, on the other hand, are caused by the presence of large obstacles between the transmitter and receiver. Fig. 2.3 illustrates the received power versus the distance, and it illustrates the path loss, small-scale fading and the large-scale fading

phenomena [17]. The small-scale fading, results in very rapid fluctuations around the mean signal level, while large-scale gives rise to relatively slow variations of the mean signal level. As for the small-scale phenomenon, several statistical models, such as Rayleigh, Nakagami-*m* and Rician distributions have been widely used to characterize it depending on some environment conditions.

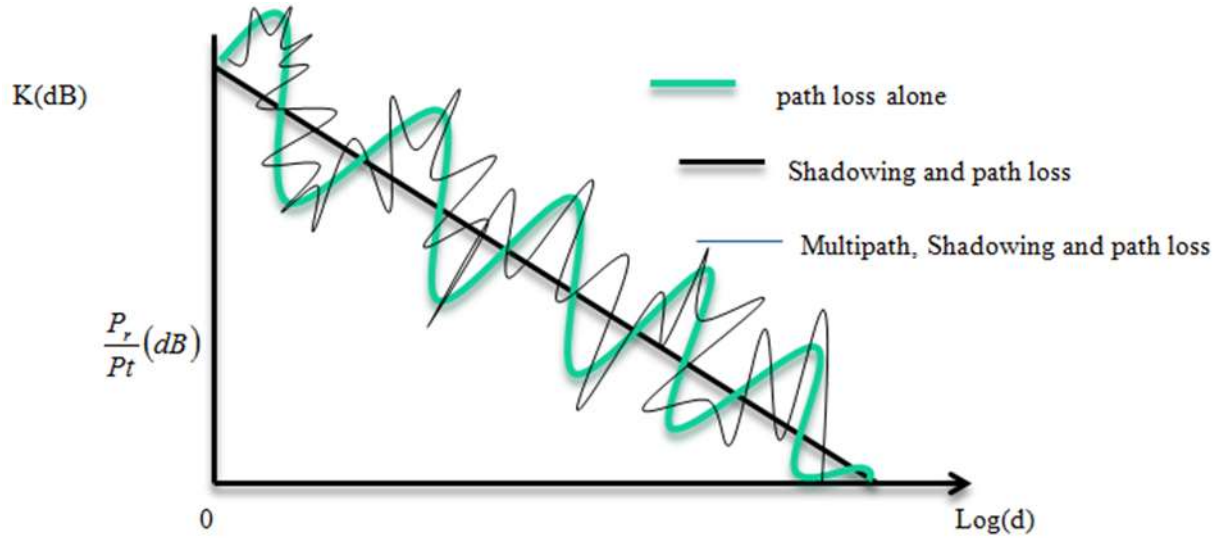

Figure 2.4 Path loss, shadowing and multipath versus distance [18]

The channel was communication medium through which the transmitted data propagates. Wireless channel is random in nature, so the signal are received from transmitter by multipath i.e. reflection, diffraction and scattering in addition to direct line of sight path [19].

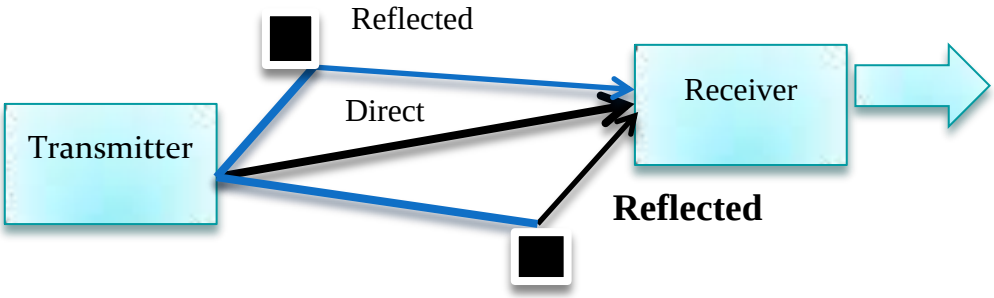

Figure 2.5 Overview of Fading Channels [20]

These phenomena include multipath scattering effects, time dispersion, and Doppler shifts that arise from relative motion between the transmitter and receiver. As shown figure 2-4 direct and

major reflected paths between a stationary radio transmitter and a moving receiver. The shaded shapes represent reflectors such as buildings

The major paths result in the arrival of delayed versions of the signal at the receiver. In addition, the radio signal undergoes scattering on a local scale for each major path. Such local scattering was typically characterized by many reflections by objects near the mobile. These irresolvable components combine at the receiver and cause a phenomenon known as multipath fading. Due to this phenomenon, each major path behaves as a discrete fading path [21].

Typically, the fading process is characterized by a Rayleigh distribution for a non-line-of-sight path and a Rician distribution for a line-of-sight path Nakagami multipath distribution offers a better fit for a wider range of fading conditions in wireless communication and Weibull indoor and outdoor communication. The relative motion between the transmitter and receiver causes Doppler shifts. Local scattering typically comes from many angles around the mobile. This scenario causes a range of Doppler shifts, known as the Doppler spectrum. The maximum Doppler shift corresponds to the local scattering components whose direction exactly opposes the trajectory of the mobile [22].

In probability theory, the set of all possible outcomes of a random trial was called sample space. Random variable was a real-valued function which was defined on the sample space. The cumulative distribution function (CDF) of a random variable X was a function $F_X(x): \Re \rightarrow [0,1]$ defined follows:

$$F_X(x) = P\{X \leq x\} \quad (2.1)$$

Where $P(x)$was the probability of an event x. A random variable X was continuous if there was an integrable function $f_x(x): \Re \longrightarrow \Re_+$such that for all $x \in \Re$

$$F_X(x) = \int_{-\infty}^{x} f_X(w)dw \quad (2.2)$$

The function $f_x(x)$ was called probability density function. For a given random variable X, the definitions of the k^{th} raw moment, mean (expected value), variance, moment generating function, and characteristic function are all given below:

MGF and CDF are useful tools for statistical analysis. It can be seen from definitions that $\emptyset$ X(w) = MX(jw). If all raw moments of X do not exist, then certainly MX(s) does not exist but

the converse was not true. Furthermore, $\emptyset$ X(w) always exists and $E[X^k] = \frac{d^k M_X(s)}{ds^k}\Big| s = 0$ suppose that $\{X_j : j = 1,2,3,4 \dots \dots \dots . m\}$ was a set of m random variables. Then their joint statistical behavior was characterized by joint PDF denoted by $f(x1, x2, x3 \dots \dots \dots \dots \dots xm)$. These random variables are called independent from one another [23].

$$f(x1, x2, x3 \dots \dots \dots \dots \dots xm) = f_{X1}(x1) f_{X2}(x2) f_{X3}(x3) \dots \dots \dots \dots \dots \dots \dots \dots f_{X1}(xm) \quad (2.3)$$

And they are said identically distributed if

$$f_{X1}(x) = f_{X2}(x) = f_{X3}(x) \dots \dots \dots \dots \dots \dots \dots \dots \dots f_{Xm}(x) \quad (2.4)$$

Variables can be both independent and identically distributed (iid).Function of a random variable provides another random variable with its own PDF. Suppose g was an invertible and monotonically function of a single random variable X such thatY = g(w). Then the PDF of Y in terms of the PDF of X was given by

$$F_Y(y) = \left|\frac{d}{dy} g^{-1}\right| f_x\left(g^{-1}(y)\right) \quad (2.5)$$

The maximum and minimum of a given set of random variables $\{X_j : j = 1,2,3,4 \dots \dots \dots . m\}$are also random variables. If Xmax denotes the maximum and Xmin denotes the minimum, then the following equations are valid for the two random variables [24].

$$P\{X_{max} \leq x\} = P\{X_1 \leq x, X_2 \leq x, X_3 \leq x \dots \dots \dots \dots \dots X_m \leq x\} \quad (2.6)$$

$$P\{X_{min} \geq x\} = P\{X_1 \geq x, X_2 \geq x, X_3 \geq x \dots \dots \dots \dots \dots X_m \geq x\} \quad (2.7)$$

In digital communication, signal from an information source, communication channel and noise generated at the receiver are usually random and functions of time. At any given time instant, the value of each of them was random variable. Therefore, they can be characterized by a collection of random variables which was called as random process or stochastic process.

2.4. Wireless channel

The performance of any communication system over radio channel is a basic element that is looked into when selecting a specific transmission technique for any application or large-scale deployment. It is usually evaluated in terms of average signal-to-noise ratio (SNR), outage probability and bit error probability (alternatively bit error rate (BER)). Except for a few specific applications related to air interface transmission techniques, fading, shadowing, reflection, refraction, scattering, diffraction and the like processes are considered as unfavorable phenomena when occurring in radio interface. In addition, channel capacity is limited by

available bandwidth as well [25]. Effects due to path loss, the Doppler spread and multipath propagation are also to be accounted when providing solutions for problems associated with any type of communication technique. These effects are capable of generating additional forms of interferences like inter-symbol interference (ISI), inter-carrier interference (ICI) and a combination of inter-carrier and inter-symbol interference (ICSI). In other words channel characteristics are dependent on multipath fading, the rate of time variation and frequency selectivity. Due to these reasons, air interface is still identified as one of the bottlenecks in mobile and wireless communication, basically in terms of capacity and reliability [26].

There are four types of fading. They are determined by the bandwidth and symbol period of the transmit signal. When the signal bandwidth was smaller than the coherence bandwidth of the channel, the channel is said to be flat-faded or frequency-flat. Otherwise it is said to exhibit frequency-selective fading. When the symbol period is much shorter than the coherence time, the channel is defined as slow fading. Otherwise, the channel is regarded as fast fading [27]. Frequency-selective fading was seen in high-data rate transmissions. This is due to the wider bandwidth of the transmit signal than bandwidth over which the frequency response of a wireless channel has a constant gain and linear phase. In other words, this is a phenomenon caused by the time dispersion of the transmit symbol within the channel [26-27].

2.4.1. Multipath Propagation

Multipath propagation is one of the main phenomenon in a wireless channel. Different replicas of the transmit signal are received through different paths and have distinct properties like distance and attenuation strengths. The delays and the channel coefficient values vary, generating delay and Doppler spreads. The most important parameters of a channel are coherence bandwidth and coherence time. Coherence bandwidth is a statistical measure of the range of frequencies over which a channel can be considered to be flat. Or coherence bandwidth may be the approximate maximum bandwidth or frequency interval over which a comparable or correlated amplitude fading is likely to be experienced by two frequencies of a signal. Again, this is reciprocal to the multipath spread. There may be constructive or destructive contributions to the total signal, due to these replicas of the transmit signal, leading to rapid fluctuations of

the resultant signal at the receiver [28].

2.4.2. Inter-symbol Interference

Basically, signals arriving through delayed paths as copies of the transmit signal are not helpful for signal detection. They are identified as ISI and make the communication systems less reliable. Most of the time these replicas have less signal power than does the first arrive signal. Here ISI is a form of signal distortion where one symbol interferes with the subsequent symbols. Further, ISI is a resultant of multipath propagation and frequency-selective fading of the wireless channel. The other main reason for ISI is the transmission of signal through a bandlimited channel. In this situation, the frequency response above a certain frequency known as the cutoff frequency is zero. Signals passed outside the band are removed, leading to a new pulse shape for the receive signal [29]. A symbol can be spread over the subsequent symbol periods, due to a change in its pulse shape. Apart from the loss incurred due to the change of the shape of the first symbol, other symbols can also be subjected to severe interference. When a message is transmitted through such channel, the spread pulse of each individual symbol will interfere with the subsequent symbols [29-30]. Pulse shaping can be used to avoid interference caused by bandwidth limitation. If a channel frequency response is flat and the shaping filter is with a finite bandwidth, it is possible to communicate without generating any ISI at all. In the design of the transmit and receive filters, attempts are always made to minimize the effects of ISI in general, irrespective of their causes. Other widely used remedial methods to compensate ISI include the use of adaptive equalizers. Channel codes (error correction codes) can also be used to combat ISI or to improve the link performance in the case of imperfect channel equalization. Some communication techniques, mainly in the family of multicarrier communication techniques, are, by design alone, quite robust against ISI. Unfortunately, FBMC is highly susceptible in this respect [30].

2.4.3. Large scale fading

According to radio signal propagation there was two types of fading; large scale fading and small scale fading. Large scale fading represents average attenuation, amplitude and phase shift changes or path loss due to motion of the large areas. This phenomenon affected by prominent earth objects (tress, building, hills, forests etc.) between the transmitter and the receiver, the receiver was often represented as being shadowed by such prominent. Due to which a great variation occur in the strength of the received signal. The measured signal power differs substantially at different locations even though at the same radial distance from a transmitter.

These Represents the medium scale fluctuations of the radio signal strength over distances from tens to hundreds of meters. Average powers now when the phenomena of large scale fading occur then this value deviates from the mean average value [31].

2.4.4.Medium scale fading

Shadowing was a medium-scale effect field strength variations occur if the antenna was displaced over distances larger than a few tens or hundreds of meters. It was the effect that the received signal power fluctuates due to objects obstructing the propagation path between transmitter and receiver. These fluctuations are experienced on local mean powers, that was, short-term averages to remove fluctuations due to multipath fading. In an area where signal reception would normally be strong, certain other factors may have an effect on the reception, thereby making it either stronger or weaker, or may cause complete RF interference. Like a building with thick walls or of mostly metal construction (or with dense rebar in concrete) may prevent a mobile phone from being used. Underground areas, such as tunnels and subway stations, lack reception unless they are wired for cell signals. There may also be gaps where the service contours of the individual base stations of one's mobile carrier (and/or its roaming partners) do not completely overlap [32].

2.4.5. Small scale fading

Small-scale fading refers to the dramatic changes in signal amplitude and phase that can be experienced as a result of small changes in the spatial separation between a receiver and transmitter. For mobile radio applications, the channel was time-variant because motion between the transmitter and receiver results in propagation path changes. The rate of change of these propagation conditions accounts for the fading rapidity (rate of change of the fading impairments). Small-scale fading was also called Rayleigh fading because if the multiple reflective paths are large in number and there is no line-of-sight signal component, the envelope of the received signal is statistically described by a Rayleigh PDF. When there is a dominant non fading signal component present, such as a line-of-sight propagation path, the small scale fading envelope is described by a Rician PDF. A mobile radio roaming over a large area must process signals that experience both types of fading: small-scale fading superimposed on large-scale fading [31-32].

2.4.6. Flat fading

If a channel has a constant response for a bandwidth greater than the transmitted signal bandwidth, then the channel was said to be a flat fading channel. The conditions for a flat fading channel are: $B_s \leq B_c$ $T_s \geq T_c$

Doppler spreads are negligible where Bs and Ts are the signal bandwidth and the symbol duration respectively. The term 'Flat' indicates that all frequencies of the transmitted signal experience the same level of channel gain (or attenuation). The transmitted spectrum was preserved at receiver. The channel gain was fluctuating with time, and so was the received signal strength. Because the symbol period (Tb) is reciprocal of signal bandwidth, it follows that it must be much larger than the rms delay spread of the channel, which was inversely proportional to the channel coherence bandwidth (Bc). This type of fading channel was sometimes referred to as a narrow-band channel [33].

2.4.7. Frequency selective fading

On the other hand, if the bandwidth of the transmitted signal was much larger than the channel coherence bandwidth, frequency selective fading occurs. In this case, the channel gain was not only fluctuating in time, but was also different for different frequency components of the transmitted signal. This type of fading channel is more severe than flat fading channel, as it induces Inter Symbol Interference (ISI).

$$B_s \leq B_c \qquad T_s \geq T_c$$

The concept of pulse-shaping is used to control the transmit signal bandwidth [14].

2.4.8. Fast fading

Depending on how rapidly the transmitted signal changes compared to the rate of change of the channel, a channel may be classified either as fast fading or slow fading. In the fast fading channel, the channel characteristics are changing rapidly within the symbol duration. It means that the channel coherence time (Tc) is smaller than the symbol period (Tb). As the channel coherence time is inversely proportional to the Doppler spread (Bd), the fast fading channel often has high Doppler spread. In practice, fast fading only occurs for very low data rate transmission [34].

2.4.9. Slow fading

In contrast, if the channel impulse response changes at a rate much slower than the symbol rate, the channel is said to be 'slow fading'. Such channel was assumed to be static over one or several symbol periods (Tb). In frequency domain, this implies that the Doppler spread (BD) of the channel was much less than the bandwidth of the transmitted baseband signal [33-34].

2.4.10. **Doppler spread**

Doppler spread which means it describes the time dispersive nature of the channel in a local area network. Doppler spread was a measure of the spectral broadening caused by the time rate change of the mobile channel, also defined as the range of the frequency over which the received Doppler spread was essentially non zero. The amount of spectral broadening depends on fd which is a function of the relative velocity of the mobile, and the angle θ between the direction of motion of the mobile and direction of arrival of the scattered waves. If the baseband signal bandwidth is much greater than Bd the effects of Doppler spread are negligible at the receiver. This was a slow fading channel [35]. The Doppler Effect is caused by a shift in the receive signal frequency from that of the original transmit frequency due to differences in relative velocities. The Doppler shift range across the bandwidth of the signal is known as the Doppler spread. The value of the Doppler spread can be considered as a measure of how rapidly the channel impulse response varies in time. Typically, the reason for that is the relative movement between the source and the destination nodes. The coherence time of a channel denotes the period of time within which the channel fading remains correlated above a predetermined threshold. The coherence time is inversely proportional to the Doppler spread. Thus, a slowly fading channel has a large coherence time and a fast fading channel has a small coherence time.

2.4.11. Additive White Gaussian Noise Mode (AWGN)

The simplest radio environment in which a wireless communications system or a local positioning system or proximity detector based on Time of-flight will have to operate was the Additive-White Gaussian Noise (AWGN) environment. Additive white Gaussian noise (AWGN) was the commonly used to transmit signal while signals travel from the channel and simulate background noise of channel. The mathematical expression in received signal $r(t) = s(t) + n(t)$that passed through the AWGN channel where s (t) was transmitted signal and n (t) is background noise.

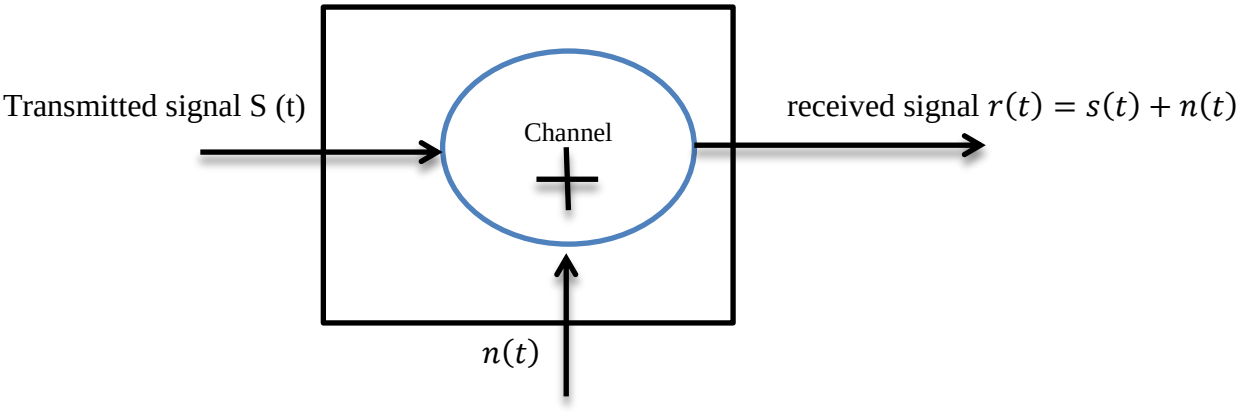

Figure 2.6 Block diagram of AWGN Channel model [37]

An AWGN channel adds white Gaussian noise to the signal that passes through it. It was the basic communication channel model and used as a standard channel model. The transmitted signal gets disturbed by a simple additive white Gaussian noise process [36].

2.5. Distributions for Fading

2.5.1. Gaussian/Normal Distribution

Let X be a random variable that follows Gaussian distribution with parameters σ and μ (usually denoted X ~N (μ ; σ^2)). Then its PDF, CDF, MGF (moment generating function), Mean and Variance given table 3.1. In the error function was defined

$$f_X(x) = \frac{1}{\sigma\sqrt{2\pi}} e^{\frac{-(x-\mu)^2}{2\sigma^2}} \quad (2.8)$$

$$F_X(x)\ \frac{1}{2}\left[1 + erf\left(\frac{x-\mu}{\sigma\sqrt{2}}\right)\right] \quad (2.9)$$

$$E[x^k] = \left(-i\sigma\sqrt{2}.sgn(\mu)^k U\left(\frac{-k}{2}, \frac{1}{2}, \frac{-\mu^2}{2\sigma^2}\right)\right) \quad (2.10)$$

$$M_X(s) = e^{\mu s + \frac{1}{2}\sigma^2 s^2} \qquad E[X] = \mu, \quad VAR[X] = \sigma^2 \quad (2.11)$$

Table 2-1 CHARACTERIZATION OF GAUSSIAN DISTRIBUTION [38]

By relation

$$erf(z) = \frac{2}{\sqrt{\pi}} \int_0^z e^{-t^2} dt \quad (2.12)$$

In the real axis, $erf(-\infty) = -1;\ erf(0) = 0;\ erf(\infty) = 1 and\ erf(-x) = -erf(x)$.The general formula for the raw moments of X was complicated due to the conuent hypergeometric function, but the moments can be computed easily for small values of k using the formula

$$E[X^k] = \frac{d^k M(s)}{ds^k} \tag{2.13}$$

Furthermore, the central moments are

$$E[(x-\mu)^n] = \begin{cases} \dfrac{(2k)!\,\sigma^{2k}}{2^k k!} & for\ n = 2k \\ 0 & for\ n = 2k-1 \end{cases} \tag{2.14}$$

The distribution fulfills the following properties [39]

If $X \sim N(\mu, \sigma^2)\ and\ a, \in R\ then\ ax + b \sim N(a\mu + b, a^2\sigma^2)$ If $\{X_i, i = 1,2 \dots \dots n\}$ are independent variable such that $X_i \sim N(\mu_i, \sigma^2)$ then $\sum_{i=1}^{n} X_i \sim N\left(\sum_{n=1}^{N} \mu_i \sum_{n=1}^{N} {\sigma_i}^2\right)$ this distribution was used as a model for many complex phenomena in various fields of science.

2.5.2. Rayleigh Fading Channel

Rayleigh fading was considered as the most effective model for tropospheric and ionospheric signal propagation, as well as the effect of heavily built up urban environment on radio signals.

$$f_X(x) = \begin{cases} \frac{x}{\sigma^2} e^{\frac{-x^2}{2\sigma^2}} & x > 0 \\ 0 & x \le 0 \end{cases} \tag{2.15}$$

$$F_X(X) = \begin{cases} 1 - e^{\frac{-x^2}{2\sigma^2}} & x > 0 \\ 0 & x \le 0 \end{cases} \tag{2.16}$$

$$E\left[X^k\right] = (2\sigma^2)^{\frac{k}{2}} r\left(\frac{k}{2} + 1\right) \tag{2.17}$$

$$M_X(s) = M\left(1, \frac{1}{2}, \frac{1}{2}\sigma^2 s^2\right) + \sqrt{\frac{\pi}{2}} \sigma s e^{\frac{1}{2}\sigma^2 s^2} \tag{2.18}$$

$$E[X] = \sigma\left(\sqrt{\frac{\pi}{2}}\right) \tag{2.19}$$

$$VAR[X] = \left(\frac{4-\pi}{2}\right)\sigma^2 \tag{2.20}$$

Table 2-2 CHARACTERISTICS OF RAYLEIGH DISTRIBUTION [40-41]

Rayleigh fading is considered when there was no line of sight communication between the transmitter and receiver. If there is much scatter in the environment that scatter the radio signals before it arrives at the receiver, then in this case central limit theorem holds. Let $\{X_i, i = 1,2 \ldots\ldots n\}$ be iid zero mean Gaussian random variables such that $X \sim N(0,\sigma^2)\ \forall i$. Then $X = \sqrt{\sum_{i=1}^{n} X_i{}^2}$ is defining as a generalized Rayleigh random variable when n = 2 in the equation, we get the Rayleigh distribution. Its PDF, CDF, MGF, raw moments, mean and variance are given in table 2.2 Rayleigh distribution is used to model small-scale fading in wireless communication channel when the channel was characterized by a large number of scatters and there was no dominant path or a line of sight connection. For instance, urban areas in mobile communication mostly have this kind of channel [40]

According to central limit theorem of the baseband equivalent impulse response of a channel with a large number of scatters can be modeled by a zero mean complex Gaussian process. Therefore, the envelope of the channel impulse response was the square roots of the sum of the squares of two zero mean Gaussian random processes. By definition, this process was Rayleigh. Furthermore, based on extensive measurements of the envelope of the received signal at the receiver, suggested Rayleigh process as a suitable model in urban and suburban areas [41].

2.5.3. Rician fading channel

Rician fading model was applicable most when in addition to scattering there was a strongly dominated signal was seen at the receiver, usually caused by line of sight. During such random process, mean will no longer be zero. In this case mean will vary around the power level of the dominant path. Let $\{X_i, i = 1, 2.....n\}$ be independent Gaussian random variables with same variance but different mean such that $\sim N(0,\sigma^2)$, $\forall i$. Then $X = \sqrt{\sum_{i=1}^{n} X_i{}^2}$ was defined as a generalized Rician random variable. When n = 2 in the equation, we get the Rician distribution. In what follows, we denote $a = \sqrt{\sum_{i=1}^{n} X_i{}^2}$ The Rician distribution descriptions are given in Table 2.3**.** Rice process was chosen as a suitable model of wireless channel when there was a dominant path or line of sight connection between the transmitter and receiver. Rural areas in mobile communication, for instance, usually possess this kind of channel. In the presence of a dominant

or line-of-sight component, we get the sum of the scattered components and line of sight components at the receiver [42]. According to central limit theorem the baseband equivalent of the sum was a complex Gaussian process. Furthermore due to the dominant path, the mean of the real part was different from zero. So the envelope of the impulse response was a Rice process. The situation was similar with a sinusoidal wave plus random noise which has been treated by Rician.

$f_X(x) = \begin{cases} \frac{x}{\sigma^2} e^{\frac{-x^2-a^2}{2\sigma^2}} I_o\left(\frac{ah}{\sigma^2}\right) & x > 0 \\ 0 & x \le 0 \end{cases}$	(2.21)
$F_X(x) = \begin{cases} 1 - Q_1\left(\frac{a}{\sigma}, \frac{x}{\sigma}\right) & x > 0 \\ 0 & x \le 0 \end{cases}$	(2.22)
$E[X^k] = (2\sigma^2)^{\frac{k}{2}} e^{\frac{-a^2}{2\sigma^2}} \Gamma\left(1 + \frac{k}{2}\right) M\left(1 + \frac{k}{2}, 1, \frac{a^2}{2\sigma^2}\right)$	(2.23)
$E[X^2] = 2\sigma^2 + a^2$	
$E[X] = a\sqrt{\frac{\pi}{2}} M\left(-\frac{1}{2}, 1, \frac{-a^2}{2\sigma^2}\right)$	(2.24)
$VAR[X] = E[X^2] - (E[X])^2$	(2.25)

Table 2-3 CHARACTERIZATION OF RICIAN DISTRIBUTION [41-42]

In addition, the analysis based on experimental data in shows that Rician distribution was more accurate than Rayleigh, Nakagami and Weibull distributions in modeling the signal statistics in rural areas [43].

2.5.4. Nakagami fading channel

The Nakagami-m fading channel model has been widely used to model the fading distribution in various wireless channels. While the Rayleigh and Rice distributions can indeed be used to model the envelope of fading channels in many cases of interest, it has been found experimentally that the Nakagami distribution offers a better fit for a wider range of fading conditions in wireless communications. Since the value of k was an indicator of the severity of the fading channel conditions and influences the BER, the knowledge of its values range can be used in the evaluation and design of different wireless communications techniques [44]. The Nakagami fading provides a very good fit for all fading conditions ranging from very severe to no fading because of the presence of an adaptive fading parameter 'm' called shape

factor. A Nakagami-distributed random variable X was characterized by Table below 2.4. In Table below the following notations are used: $\Omega = E[X^2]$ and$m = \frac{\Omega^2}{E[(X^2-\Omega)^2]}$Parameter m was usually called fading figure and the distribution is defined only for $m \geq .\frac{1}{2}$.The incomplete gamma function needed in Table 2.4 is defined as

$$\gamma(u,x) = \int_0^x t^{u-1}e^{-t}dt \tag{2.26}$$

Nakagami distribution does not have a general closed form MGF. Nakagami random variable becomes a Rayleigh random variable when m =1

$f_x(x) = \begin{cases} \frac{2}{\Gamma(m)}\left(\frac{m}{\Omega}\right)^m x^{2m-1} e^{\left(\frac{-mx^2}{\Omega}\right)} & x > 0 \\ 0 & x \leq 0 \end{cases}$	(2.27)
$F_x(x) = \begin{cases} \gamma\left(m,\frac{m}{\Omega}x^2\right) & x > 0 \\ 0 & x \leq 0 \end{cases}$	(2.28)
$E[x^k] = \Gamma\left(\frac{m+k/2}{\Gamma(m)}\right)\left(\frac{m}{\Omega}\right)^{\frac{k}{2}}$	(2.29)
$E[X] = \Gamma\left(\frac{m+1/2}{\Gamma(m)}\right)\left(\frac{m}{\Omega}\right)^{\frac{1}{2}}$	(2.30)
$VAR[X] = \Omega\left(1 - \frac{1}{m}\left(\Gamma\left(\frac{m+\frac{1}{2}}{\Gamma(m)}\right)\right)\right)$	(2.31)

Table 2-4 CHARACTERIZATION OF NAKAGAMI DISTRIBUTION [45].

Furthermore, Nakagami PDF possesses larger tails than Rayleigh PDF when $\frac{1}{2} \leq m \leq 1$but the reverse was true when m > 1. Where $\Gamma(.)$the gamma function, Ω and m are the parameters of the distribution and where Ω is the average received power and m is the shape factor. The Nakagami distribution includes the Rayleigh distribution for m=1 and one-side of the Gaussian distribution for m $= \frac{1}{2}$. When m approaches infinity, it implies that there is no fading

2.5.5. Weibull fading channel

The Weibull distribution, which was also commonly used in reliability engineering and survival analysis, was shown to provide an excellent fit for indoor and outdoor environments.

Let X is a random variable that follows a 2-parameter Weibull Distribution with a scale parameter $\sigma > 0$ and a shape parameter $\beta > 0$. Then, it is characterized by table 2.5 for $\Gamma(z)$. Though there was no general closed-form solution found for the MGF, it is given in power series form in Table 2.5 since all the raw moments are known [46].

$$f_X(x) = \begin{cases} \frac{\beta}{\alpha}\left(\frac{x}{\alpha}\right)^{\beta-1} e^{-\left(\frac{x}{\alpha}\right)\beta} & x > 0 \\ 0 & x \leq 0 \end{cases} \quad (2.32)$$

$$F_X(x) = \begin{cases} 1 - e^{-\left(\frac{x}{\alpha}\right)\beta} & x > 0 \\ 0 & x \leq 0 \end{cases} \quad (2.33)$$

$$M_X(s) = \sum_{n=0}^{\infty} \frac{s^n \alpha^n}{n!} \Gamma\left(1 + \frac{n}{\beta}\right) \quad (2.34)$$

$$E(x^k) = \alpha^k \Gamma\left(1 + \frac{k}{\beta}\right) \quad (2.35)$$

$$E[X] = \alpha\Gamma\left(1 + \frac{1}{\beta}\right) \quad (2.36)$$

$$VAR(X) = \alpha^2 \left[\Gamma\left(1 + \frac{1}{\beta}\right) - \Gamma^2\left(1 + \frac{1}{\beta}\right)\right] \quad (2.37)$$

Table 2-5 CHARACTERIZATION OF WEIBULL DISTRIBUTION [47-48]

Moreover, it has also other closed-form expressions when the shape parameter β is integer or rational. When $\beta = 1$, a Weibull PDF reduces to the exponential PDF, and when $\beta = 2$, it reduces to the Rayleigh PDF [47]. Weibull distribution is another mathematical model for small-scale fading in wireless communication. Empirical studies have shown that Weibull distribution was an effective model of both indoor and outdoor propagation. Furthermore, reference describes Weibull Distribution as a less complex and accurate description for the outdoor multipath fading channel than some of the other existing models [48].

Chapter Three: System Model

3.1. Mathematical analysis of Channel Model with UFMC

UFMC waveform was a derivative of OFDM waveform combined with post-filtering, where a group of carriers was filtered by using a frequency domain efficient implementation [49]. The filtering operation leads to a lower out-of-band leakage than for OFDM. The UFMC transmitter is composed of B sub-band filtering that modulate the data blocks. The transmitted signal uses no CP, but there was still a spectral efficiency loss due to the time transient (tails) of the shaping filter. The Rx stage was composed of a 2NFFT point FFT, which was decimated by a factor 2 to recover the data. A windowing stage can also be inserted before the FFT. It introduces interference between carriers but interesting to consider for asynchronous uplink transmissions as it helps to separate contiguous users [50].

Fading channel was a communication channel comprising fading. In wireless systems fading may occur due to multipath propagation .The presence of reflectors and obstacles in the path of propagation causes multipath propagation, which creates multiple paths for transmitted signal. As a result, receiver receives superposition of multiple copies of transmitted signal. Each signal copy will experience differences in attenuation, delay and phase shift while travelling from transmitter to receiver [51].

This will result in amplifying or attenuating the signal power at receiver. Sometimes fading may be deep which causes temporarily failure of communication due to several drops in the channel Signal to Noise Ratio (SNR). Mathematically, fading was a time varying random change in amplitude and phase of transmitted signal. In wireless communication system channel fading was the degrading feature. In this chapter, the performance analysis of UFMC system was discussed over AWGN, Rayleigh fading, Rician fading and Nakagami fading channel. Probability distribution was an essential tool for a detailed understanding of statistical channel modeling. Therefore, this chapter first covers the required basics of probability theory and then it proceeds to a detailed description of distributions that are used to model fading channel. Finally, with the help of the distribution tools, statistical fading channels modeling was discussed and analyzed in detail [52]. UFMC is an intermediate waveform modulation technique between FBMC & OFDM as it filters the modulated subcarriers on a sub band basis differing from FBMC

which filters each subcarrier individually and OFDM which filters whole band at once. This filtering avoids OOB spectral emissions. In UFMC the whole sub band is sub divided into multiple sub bands of definite size, the symbols of sub bands are then passed through N -point IFFT block that modulates the symbols generating time domain samples of length N, is then passed through FIR filter of length L generating output signals of length N+L-1 as a result of the linear convolution operation. These N+L-1 signals belonging to different sub bands are added to generate final output corresponding to whole band. At the receiver, the received signal is first converted to the base band frequencies then sampled. The received signal of length N+L-1 samples cannot be demodulated by N-point FFT ,rather it is zero padded with N-L+1 zeros in order to demodulate using 2N-point FFT. The even index of total 2N generated complex values of subcarriers contains data; while the odd subcarrier contains interference from the data symbols are further discarded. Hence the way it avoids inter-symbol interference without adding cyclic prefix as of OFDM, which in turn increases spectral efficiency. A Chebyshev window with side lobe attenuation which is parameterized is employed to filter the IFFT /FFT outputs (sub bands).

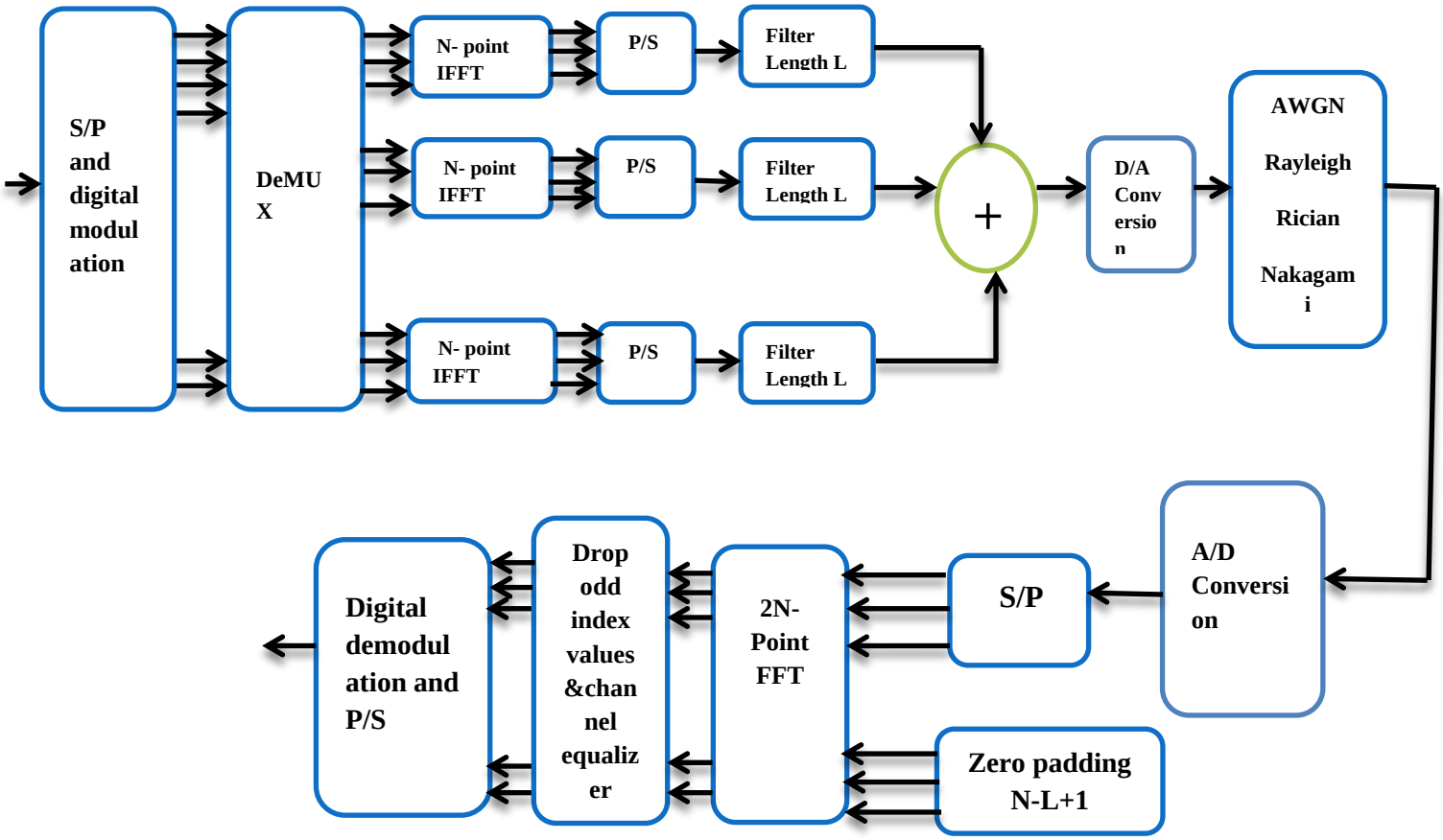

Figure 3.1 System model of UFMC [53]

As mentioned before, UFMC is considered as an intermediate technique between OFDM and FBMC as it filters the modulated subcarriers on a sub-band basis differing from FBMC which filters each subcarrier individually and OFDM which filters the whole band at once. To get a better insight of UFMC system operation, we can refer to Fig.3.1 which presents a system model of a typical UFMC system including the transmitter, channel and the receiver. Starting with the transmitter blocks, we can see that UFMC starts with subdividing the whole band into multiple sub-bands of definite size, the symbols of each sub-band are then passed to an N-point IFFT block that modulates the symbols generating time domain samples representing the modulated signal that has a length of N samples, each one of these time domain signals of length N is then passed through a digital FIR filter of length L generating an output signal of length N+L-1 as a result of the linear convolution operation. These time-domain output signals of length N+L-1 belonging to different sub-bands are all added together to generate the final output signal corresponding to the whole band. This output baseband signal is finally converted to an analog signal to be up converted and sent to the antenna.

Transmitter operation is mathematically formulated in (3.1).

$$y(n) = \sum_{i=1}^{B} x_i\,(n) * f_i(n) \tag{3.1}$$

where, i represents the index of different sub-bands, B is the total number of sub-bands and fi(n) is the impulse response of the FIR filter used with sub-band i. After passing through the channel whose effects will be clarified in details in the next section, the received signal at the receiver will be first down converted to the baseband frequencies then sampled. Assuming a single tap channel and keeping the system sampling frequency unchanged, the received digital signal whose length is N+L-1 samples cannot be demodulated by an N-point FFT operation, rather, it is zero padded with N-L+1 zeros in order to be demodulated using a 2N-point FFT where; the odd index values of the total 2N generated complex values are further discarded in order to reject the extra frequency samples taken between the peaks of the neighboring subcarriers leading to a final output of N complex valued symbols corresponding to those generated by the transmitter. The receiver operation can be similarly formulated as in (3.2). The input data represented by X is

converted sub a band is passed through N point IFFT representing with matrix V. Finally passed through filter of matrix F(s) for the i^{th} sub band

$$Y(k) = \sum_{n=0}^{N-1} Y(n) e^{\frac{-2\pi nR}{2N}} \quad (3.2)$$

It can be observed from (appendix B), $c(l', k')$ if the filter length is L = 1, which corresponds to OFDM systems. The correlation between different subcarriers in UFMC results from the Leakage effect of FFT if the FFT size is not an integer multiple of the signal length.

First, $2NL_{2,k}$ zeros are appended at the end of yk to generate vector ỹk with length 2N. Then 2Npoint DFT is performed on ỹk, followed by down-sampling by a factor of 2. This implementation, however, will introduce ISI/ICI in one-tap channel equalization in two scenarios. First scenario is in multi-path fading channels where ISI will occur due to the lack of guard interval between symbols. Even with CP added, the original UFMC system cannot achieve interference-free one-tap equalization either since the circular convolution property is destroyed.

Secondly, the implementation of 2N-point DFT operation implies that the filter length plus the channel length is smaller than N in order to make $2N - L2, k \geq 0$. However, it is not necessary to limit the system design with this constraint in general. To achieve interference-free one-tap equalization, we make the following proposition for the UFMC system [56]

$$SNR^{ofdm} = \frac{N}{L_{2,k}} . \frac{\rho_{sym}{}^{2} .}{\sigma^2} . \rho_{CH,k}{}^{2} \qquad for\ n\epsilon \cup \quad (appendix\ C) \quad (3.3)$$

It can be concluded that UFMC is a generalized OFDM system. In addition, equation (3.3) confirms that the SNR of the n-th subcarrier is independent of its location in a subband and subband index itself. Therefore, the subband index {.} m and subcarrier index n are omitted in the sequel. In order to present an overall view of the system performance in comparison to OFDM system, we focus on the average performance in one subband, in terms of output SNR, capacity and BER [62]. The frequency selectivity of the filter is the essence of the UFMC system design to make the system well-localized in the frequency domain to combat multipath channel and reduce the OoB emission. However, similar to the side effects of the channel frequency selectivity, the filter frequency selectivity may cause system performance loss, as

analyzed in the following proposition. The conclusion can be extended to system capacity without considering the overhead in high SNR region. Consider an UFMC system with

$L_{F,m} > 1$ and assume the parameters for the k-th user satisfy (appendix B). In addition, we assume the subband bandwidth is small enough to be within the coherence bandwidth. In the high-SNR region, i.e., SNR(n) >> 1, the UFMC system experiences performance loss in terms of average capacity per subcarrier in the m-th subband in comparison to the OFDM system, i.e.,

$$C_{mUFMC} \approx \frac{1}{N_m} E\left[\sum \log_2\left(SNR(n)\right)\right] \tag{3.4}$$

Now we analyze the BER performance of quadrature amplitude modulation (QAM) schemes. The BER for M_{mod}-QAM can be calculated as [63]

$$BER = 2\left(1 - \frac{1}{\sqrt{M_{mod}}}\right) Q\left(\sqrt{\frac{3SNR(n)}{M_{mod} - 1}}\right) \tag{3.5}$$

The calculation of analytical BER expression in complex due to the Q-function Q(.). thus we use the following aproximation of the Q-function as proposed

$$Q(x) \approx \frac{1}{12} e^{-\frac{x^2}{2}} + \frac{1}{6} e^{-\frac{x^2}{3}} \tag{3.6}$$

3.1. Statistical Model for Fading Channel

The transmitted signal x (t) was multiplied by the complex channel hc and then AWG noise with a one-side power spectral density No is added at the receiver to give $r(t)$.

$$\mathrm{R(t)} = \mathrm{hc} * \mathrm{x(t)} + \mathrm{n(t)} \tag{3.7}$$

Where, at time *t*, *r* (*t*) and *x* (*t*) are the received and transmitted signals respectively and *n* (*t*) is the noise, represented as a sample function from a Gaussian random process with zero mean and variance. The noise *n* (*t*) is assumed to be independent of the signal *r* (*t*). The fading channel was usually modeled with Rayleigh, Rician, Nakagami, Weibull, or/and lognormal distribution depending on the nature of the radio propagation environment. If Es was the signal energy per transmitted symbol, then the instantaneous SNR at the receiver which we denote by γ is given as

$$\gamma = \mathrm{h}^2 \frac{\mathrm{Es}}{\mathrm{No}} \tag{3.8}$$

Where$h = |hc|$. Note that h was the amplitude of the complex channel hc and we will use the notations throughout the thesis accordingly. Then the expected SNR, denoted by $\bar{\gamma}$ was

$$\bar{\gamma} = E[\gamma] = E\left[h^2 \frac{Es}{No}\right] = \frac{Es}{No} E[h^2] \quad (3.8)$$

$$\gamma = \frac{\bar{\gamma}}{E[h^2]} \quad (3.9)$$

Notice that γ was a function of the fading channel random variable h. The PDF of h can be obtained from the previous section according to the fading channel model chosen. Then, the PDF of γ can be computed from the PDF of based on equation (2.31).

$$f_\gamma(\gamma) = \left|\frac{d}{d\gamma}\sqrt{\frac{E[h^2]}{\gamma}}\gamma\right| f_h\left(\sqrt{\frac{E[h^2]}{\gamma}}\gamma\right) = \frac{1}{2}\sqrt{\frac{E[h^2]}{\gamma\gamma}} f_h\left(\sqrt{\frac{E[h^2]}{\gamma}}\gamma\right) \quad (3.10)$$

A. Rayleigh Fading Model

As mentioned in the earlier sections, when a radio wave is propagated through a communication channel, there are different factors that affect its propagation between the transmitter and the receiver. Different statistical models have been presented which help in the modeling of communication channels. Rayleigh fading is one of the models for estimating the effect of propagation environment on a radio signal. It states that when a signal passes through a communication channel its amplitude will fade randomly, according to Rayleigh distribution [64]. Furthermore, it assumes that there is no line of sight (LOS) communication between the transmitter and the receiver and that a multipath propagation environment exists as well. If there is a strong line of sight component of the signal at the receiver, Rician may be more applicable. The mobile station antenna does not always receive the transmitted signal over LOS. It receives a number of reflected, diffracted and scattered waves as a result of multipath propagation. As a result the phases are random and ultimately, the received power also becomes a random variable. The transmitted signal with a frequency fc may reach the receiver via a number of paths, the j^{th} path having amplitude Aj, and a phase $\emptyset_j$. If we assume that there is no direct path or line-of sight (LOS) component, the received signal m (t) can be expressed as

$$m(t) = \sum_{j=1}^{N} A_j \cos(f_c + \emptyset_j) \quad (3.11)$$

where N is the number of paths. The phase $\emptyset_j$depends on varying path lengths, changing by 2π

when the path length changes by a wavelength. Therefore, the phases are uniformly distributed over [0; 2π]. When there are a large number of scatters in the channel that affect the signal at the receiver and there is no LOS between the transmitter and the receiver, Rayleigh fading is used to estimate the channel performance. Eventually the I (in phase) and Q (quadrature, out of phase) components become Gaussian distributed (by central limit theorem) and their envelope $R = \sqrt{I^2 + Q^2}$ is Rayleigh distributed. Probability density function (pdf) of Rayleigh distribution with respect to random variable r is

$$\mathrm{P_R(r)} = \frac{\mathrm{r}}{\sigma^2}\mathrm{epx}\left(\frac{-\mathrm{r}^2}{2\sigma^2}\right) \qquad (3.12)$$

Rayleigh distribution is characterized by the single parameter. Rayleigh fading channels are used to simulate high frequency communication for example, ionospheric communications. Unfortunately, it does not simulate this sort of communication with a reliable accuracy

Applicability of the Rayleigh channel fading whenever, a communication channel has to go through many scatters this means Rayleigh fading can be a useful model for that scenario. In such situations there is no LOS between the transmitter and the receiver and scatters such as buildings, trees, dust and many other objects causes attenuation, reflection, refraction and diffraction in the transmitted signal. In long distance and high frequency communication such as ionospheric and tropospheric signal propagation the particles in the atmosphere also act as scatters which can be approximated by Rayleigh fading. Rayleigh fading is a small scale effect. There are different properties of the environment for example path loss and shadowing which are superimposed by fading. The speed with which the channel fades is affected by how fast the receiver and/or transmitter are moving (Doppler Effect). Therefore, using the mean and variance expressions of Table 3.4,

$$\mathrm{E[h^2]} = \mathrm{VAR[X]} + (\mathrm{E[h]})^2 = \left(\frac{4-\pi}{2}\right)\sigma^2 + \left(\sigma\sqrt{\frac{\pi}{2}}\right)^2 = 2\sigma^2 \qquad (3.13)$$

Then using (2.15) and the PDF expression in Table 3.4, (2.15) reduces into

$$\mathrm{f_\gamma(\gamma)} = \frac{1}{\bar{\gamma}}\mathrm{e}^{\frac{-\gamma}{\bar{\gamma}}} \qquad \gamma > 0 \qquad (3.14)$$

Notice from (3.9) that γ was an exponential random variable with a scale parameter $\bar{\gamma}$

Therefore

$$F_\gamma(\gamma) = \int_{-\infty}^{\gamma} f_\gamma(w)dw = 1 - \exp\left(\frac{-\gamma}{\bar{\gamma}}\right) \qquad \text{for } \gamma > 0 \qquad (3.15)$$

$$M_\gamma(s) = \int_{-\infty}^{\infty} e^{s\gamma} f_\gamma(\gamma) d\gamma = \frac{1}{1-\bar{\gamma}s} \qquad (3.16)$$

It can also be shown that γ was a central chi-square random variable with two degrees of freedom and parameter $\sigma = \sqrt{\frac{\gamma}{2}}$

B. Rician Fading Model

Rician fading model was used to simulate environment that has a dominant line of sight path and multiple scatters components. Consider two Gaussian random variables X and Y. Here X models the line of sight component, which has non-zero mean, and Y models the randomly scatter components, which have zero mean. Both have equal variance σ^2. Then, at the receiver, all the multipath scatter signals overlays a stronger line of sight signal will produce the envelope, $R = \sqrt{I^2 + Q^2}$ which is Rician distributed. Rician fading or Rician fading was a stochastic model for radio propagation anomaly caused by partial cancellation of a radio signal by itself the signal arrives at the receiver by several different paths (hence exhibiting multipath interference), and at least one of the paths is changing (lengthening or shortening). Rician fading occurs when one of the paths, typically a line of sight signal, was much stronger than the others. In Rician fading, the amplitude gain is characterized by a Rician distribution. A Rician fading channel can be described by two parameters K and Ω. K is the ratio between the power in the direct path and the power in the other, scattered, paths. Ω is the total power from both paths $\Omega = (v^2 + 2\sigma^2)$and acts as a scaling factor to the distribution [65]. The receiving signal amplitude (not the receiving signal power) R the Rician distribution with parameter $v^2 = \frac{K}{1+K}\Omega$ and $\sigma^2 = \frac{\Omega}{2(1+K)}$the resulting Pdf then is

$$f(x) = \frac{2(K+1)x}{\Omega} \exp\left(-K - \frac{(K-1)x}{\Omega}\right) I_o\left(2\frac{\sqrt{K(K+1)}}{\Omega}x\right) \qquad (3.17)$$

Where $I(.)$ is the order of 0^{th} Bessel function of the first kind. In this model, h was considered to be Rician random variable. Therefore, from Table 2.3, we get that

$$E[h^2] = 2\sigma^2 + a^2 \quad (3.18)$$

In Rician fading channel, there is a parameter called Rician K-factor which was defined as

$$K = \frac{a^2}{2\sigma^2} \quad (3.19)$$

Then E [h^2] can also be expressed in terms of K as

$$E(h^2) = 2\sigma^2 + a^2 = 2\sigma^2\left(1 + \frac{a^2}{2\sigma^2}\right) = 2\sigma^2 \quad (3.20)$$

Using the PDF expression in Table 2.3 and (2.16), Equation (2.15) is simplified into

$$f_\gamma(\gamma) = \frac{(1+K)e^{-K}}{\overline{\gamma}}\, exp\left(-\left(\frac{1+K}{\overline{\gamma}}\right)\gamma\right) I_o\left(\sqrt{\frac{4K(1+K)}{\overline{\gamma}}\gamma}\right) \quad (3.21)$$

for I0 (z). It can be seen from (2.27) that γ was non-central chi-square random variable with parameters $\sigma = \sqrt{\frac{K\overline{\gamma}}{K+1}}$ and $\sigma = \sqrt{\frac{\overline{\gamma}}{2(K+1)}}$ therefore, using CDF and MGF expressions of non-central chi-square variable obtain.

$$F_\gamma(\gamma) = 1 - Q_m\left(\sqrt{2K}, \sqrt{\frac{1(K+1)\gamma}{\overline{\gamma}}}\right) \quad (3.22)$$

$$M_\gamma(s) = \frac{K+1}{K+1-\overline{\gamma}s}\exp\left(\frac{K\overline{\gamma}s}{K+1-\overline{\gamma}s}\right) \quad (3.23)$$

C. Nakagami-m Fading Model

Nakagami-m fading model pays lots attention on extend to its capacity to describe a wider class of fading channel conditions with better matching to empirical data than other models. Nakagami-m fading occurs when multipath scatters with relatively large delay-time spreading, with different clusters of reflected waves. The summation of multiple independent and identically distributed Rayleigh-fading signals has amplitude with Nakagami-m distribution. This was particularly relevant to model multiple sources interference. Nakagami-m distribution describes the amplitude of received signal after maximizing the diversity combination ratio. Also, Nakagami-m model is more flexible due to its adaptability fading channel conditions than the Rayleigh distribution. Whereas Rayleigh distribution was a special case of Nakagami-m when m=1. Probability density function of Nakagami-m was [66]

$$f(r) = \frac{2m^m r^{2m-1}}{\Gamma(m)\Omega^m} exp\left(\frac{-mr^2}{\Omega}\right) \quad (3.24)$$

In Nakagami fading channel model, the amplitude of the channel impulse response is considered to be Nakagami random variable. Thus, from the notation used in Table 2.4, we get

$$|hE^2| = \Omega \quad (3.25)$$

Then substituting the PDF in Table 2.4 into (3.7), the PDF of γ becomes

$$f_\gamma(\gamma) = \frac{m^m}{\Gamma(m)\gamma^{-m}} \gamma^{m-1} e^{\frac{-m\gamma}{\gamma}} \qquad \gamma > 0 \quad (3.26)$$

We can show from (3.23) that γ is gamma-distributed random variable with shape parameter and scale parameter $\frac{\overline{\gamma}}{m}$. Consequently

$$F_\gamma(\gamma) = \frac{\Gamma\left(m, \frac{m\gamma}{\gamma}\right)}{\Gamma(m)} \qquad \gamma > 0 \quad (3.27)$$

$$M_s(s) = \left(1 - \frac{\gamma s}{m}\right)^m \quad (3.28)$$

The M-ary square QAM signal is two dimensioanl generalazation of the one dimension M-ary PAM signal. The QAM signal consists of two independently amplitude modulation carriers in quadrature expression by[67]

$$s(t) = A_i cos 2\pi f_c t - A_j sin 2\pi f_c t \, , 0 \le t \le T \quad (3.29)$$

Where A_i and $A_j$are the amplitude of in-pahse and quadrature component f_c is the carrier frequency and T the symbol period. Depending on the number of possible symbols M, two distnict QAM constellation can be distingush square comnstellation with the even number of bit per symbol and rectangular constellation where the number of bits per symbol is odd.

In M-ary square QAM $\log_2 M$ bits of the serial informato=ion stream are mapped on a two-dimensional signal constellation using Gray coding . in (1) A_i and A_j are sellected independently over the set $\{\pm d, \pm 3d, \dots, \pm(\sqrt{M} - 1)d\}$ where 2d is the Euclidean distance between two adjusent signal points and given by

$$d = \sqrt{\frac{3\log_2 M.E_b}{2(M-1)}} \tag{3.30}$$

Where E_b is the bit energy. The arbitrary IxJ rectangular QAM formats consists of two QAM schemes I-art and J-ary PAM. The relation between the Euclidean distances of the nearest signal points is now

$$d = \sqrt{\frac{3\log_2(I.J).E_b}{I^2+J^2-2}} \tag{3.31}$$

Signal is transmitted from the transmitter to the receiver via channel with Nakagami-m fading. The received signal envelope can be described by Nakagami=m distribution given by (3.31)

$$P_r(r) = \frac{2m^m r^{2m-1} e^{\frac{-m}{\Omega}r^2}}{\Gamma(m)\Omega^m} \qquad x > 0, \tag{3.32}$$

Where m is the Nakagami-m parameter and Ω is the average power $\Omega = E\{r^2\}$ with E denoting mathematical expectation. On the basis of (3.32) one can show that instantaneous SNR has the gamma distribution given by

$$P_\gamma(\gamma) = \frac{m^m \gamma^{m-1} e^{\frac{m}{\Omega}\gamma}}{\Gamma(m)\Omega^m} \qquad \gamma > 0 \tag{3.33}$$

Where $\Omega = \gamma_0 = E\{\gamma\}$ is the average SNR.

D. BER analysis of QAM over the Nakagami-m fading channel

Based on (1), signal on the reception of the channel with the Nakagami-m fading is

$$S_r(t) = r.A_I cos 2\pi f_c t - r.A_J sin 2\pi f_c t, 0 \le t \le T \tag{3.34}$$

Where r is the envelope of received signal that has the Nakagami distribution given by (3.33) [68]

E. General BER expression of M-ary square QAM

Using (3.33) the conditional kth bit error probability of M- ary square QAM can be expression by

$$P_{b/\gamma}(k) =$$

$$\frac{1}{\sqrt{M}}\sum_{i=0}^{(1-2^{-k})\sqrt{M}-1}\left\{(-1)^{\left|\frac{i.2^{k-1}}{\sqrt{M}}\right|}\ x\ \left(2^{k-1}-\left|\frac{i.2^{k-1}}{\sqrt{M}}+\frac{1}{2}\right|\right)\ xerfc(2i+1)\sqrt{\frac{3\log_2 M.\gamma}{2(M-1)}}\right\} \quad (3.35)$$

Where $xerfc(.)$the complementary error is function and γ denotes the instantaneous SNR per bit. Since the instantaneous SNR per bit is random variable in order to obtain average kth bit error probability of M- ary square QAM, it is necessary to average previous expression [69]. So we have $P_b(k) = \int_{\gamma=0}^{\infty} P_{b/\gamma}(k)P_\gamma(\gamma)d\gamma$ (3.36)

Now, using (3.35) and (3.36), bit error probability $P_b(k)$ (kth bit is in error) can be expressed as

$$P_{b/\gamma}(k) = \frac{1}{\sqrt{M}}\sum_{i=0}^{(1-2^{-k})\sqrt{M}-1}\left\{(-1)^{\left|\frac{i.2^{k-1}}{\sqrt{M}}\right|}\ x\ \left(2^{k-1}\right.\right.$$

$$\left.\left.-\left|\frac{i.2^{k-1}}{\sqrt{M}}+\frac{1}{2}\right|\right)x\int_{\gamma=0}^{\infty} erfc\left((2i+1)\sqrt{\frac{3\log_2 M.\gamma}{2(M-1)}}\right)P_\gamma(\gamma)d\gamma\right\} \quad (3.37)$$

Where γ is the instantenous SNR per bit and $P_\gamma(\gamma)$ is given by (3.34). Integrating in (3.27) can be solved by representing complemantary error function and exponential function in terms of Meijer's G function by using (3.35)

$$P_b(k) = \frac{1}{M}\sum_{i=0}^{\left(1-2^{-k}\right)\sqrt{M}-1}\left\{(-1)^{\left|\frac{i.2^{k-1}}{\sqrt{M}}\right|}\ x\left(2^{k-1}-\left|\frac{i.2^{k-1}}{\sqrt{M}}+\frac{1}{2}\right|\right)x\ \frac{\left(\frac{2m(M-1)}{(2i+1)^2.3\log_2 M.\gamma o}\right)^m}{\Gamma(m).\Omega^m.\sqrt{\pi}}\right.$$

$$\left.xG_{2,2}^{1,2}\left(\frac{2(M-1)m}{(2i+1)^2 3\log_2 M.\gamma o}\middle|\begin{matrix}1-m, & \frac{1}{2}-m\\ 0, & -\ m\end{matrix}\right)\right\} \quad (3.38)$$

Using (3.33) the exact expression of average BER of M-ary square QAM is given by

$$P_b = \frac{1}{\log_2\sqrt{M}}\sum_{k=1}^{\log_2\sqrt{M}} P_b(k) \quad (3.39)$$

Where $P_b(k)$ is given by (50) [70]

F. General BER expression of M-ary rectangular QAM

In the similar way, the average BER of M-ary rectangular QAM can be determined. The average BER of IxJ rectangular QAM over Nakagami fading channel is

$$P_b = \frac{1}{\log_2(I.J)}\left(\sum_{l=1}^{\log_2 J} P_J(l)\right) \tag{3.40}$$

Where

$$P_I(k) = \frac{1}{I}\sum_{i=0}^{(1-2^{-k})I-1}\left\{(-1)^{\left\lfloor\frac{i2^{k-1}}{I}\right\rfloor} x \left(2^{k-1} - \left\lfloor\frac{i2^{k-1}}{I} + \frac{1}{2}\right\rfloor\right) \frac{\left(\frac{m(I^2+J^2-2)}{(2i+1)^2 3\log_2(IJ)\gamma 0}\right)^m}{\Gamma(m){\gamma_o}^m\sqrt{\pi}} x\right.$$

$$\left. G_{2.2}^{1,2}\left(\frac{m(I^2+J^2-2)}{(2i+1)^2 3\log_2(IJ)\gamma 0}\middle| \begin{matrix} 1-m, \frac{1}{2}-m \\ 0, \qquad -m \end{matrix}\right) \right\} \tag{3.41}$$

$$P_I(l) = \frac{1}{J}\sum_{j=0}^{(1-2^{-l})J-1}\left\{(-1)^{\left\lfloor\frac{j2^{l-1}}{I}\right\rfloor} x \left(2^{l-1} - \left\lfloor\frac{j2^{l-1}}{I} + \frac{1}{2}\right\rfloor\right) \frac{\left(\frac{m(I^2+J^2-2)}{(2j+1)^2 3\log_2(IJ)\gamma 0}\right)^m}{\Gamma(m){\gamma_o}^m\sqrt{\pi}} x\right.$$

$$\left. G_{2.2}^{1,2}\left(\frac{m(I^2+J^2-2)}{(2j+1)^2 3\log_2(IJ)\gamma 0}\middle| \begin{matrix} 1-m, \frac{1}{2}-m \\ 0, \qquad -m \end{matrix}\right) \right\} \tag{3.42}$$

[71]

G. Weibull Fading Channel

Weibull distribution was a flexible statistical model for describing multipath fading channels for both indoor and outdoor propagation environments. Experimental data supporting the Weibull fading model was reported by Shepher and Hashemi considered its use as a model for indoor fading channels. The probability density function (PDF), of the Weibull distribution are given, by

$$\mathrm{P_a(a)} = \frac{\mathrm{k}}{\Omega}\mathrm{a^{k-1}}\exp\left(\frac{\mathrm{a^k}}{\Omega}\right) \tag{3.43}$$

Where, k > 0 was Weibull fading parameter can take values between 0 and ∞. As k increases the fading severity decreases, while for the special case of k=2, reduces to the well-known Rayleigh PDF. Moreover, for the special case of k=1, Eq. (3.43) reduces to the well-known exponential PDF. Here h was a Weibull random variable. Therefore, from Table 2.5, we get that

$$E[h^2] = \alpha^2 r\left(1 + \frac{2}{\beta}\right) \tag{3.44}$$

Substituting (3.25) and PDF of h from Table 2.5 in (3.5) gives

$$f_\gamma(\gamma) = \frac{\beta}{2b\gamma}\left(\frac{\gamma}{b\gamma}\right)^{\frac{\beta}{2}-1} e^{-\left(\frac{\gamma}{b\gamma}\right)^{\frac{\beta}{2}}} \tag{3.45}$$

where $b = \frac{1}{r\left(1+\frac{2}{\beta}\right)}$ for $\Gamma(.)$. Notice from 3.58 that γ was also a Weibull random variable with a shape parameter equal to $\frac{\beta}{2}$ and scale parameter equal to $b\bar{\gamma}$. Therefore, using CDF and MGF in Table 2.5,

$$F_\gamma(\gamma) = 1 - \exp\left[-\left(\frac{\gamma}{b\gamma}\right)^{\frac{\beta}{2}}\right] \qquad \gamma > 0 \tag{3.46}$$

$$M_\gamma(s) = \sum_0^\infty \frac{(b\gamma)^n s^n}{n!} r\left(1 + \frac{2n}{\beta}\right) \tag{3.47}$$

3.2. The Measures in Fading Channels

In this chapter, some widely used performance measures in fading channels are presented. The channel fading from neighboring transmissions is considered. First, we will summarize expressions for average bit error probability (BEP) with the 32-FSK, PAM, DPSK, 16QAM, 32QAM 64QAM and 128-QAM modulation schemes in Rayleigh, Rician and Nakagami-m fading channels. Then computations and resultant expressions of performance comparison of channel model in terms of BER vs SNR.

3.2.1. Average BEP channel model under various modulation schemes

Bit error probability was one of the key performance measures in wireless communication and it was defined as the error probability in transmission of a single bit. Average BEP calculation of a wireless communication system was dependent on the modulation scheme and channel model which are used by the system. In what follows, average BEP for Rayleigh, Rician, Nakagami, and Weibull fading channel models with 32-FSK, PAM, DPSK, 16QAM, 32QAM 64QAM and 128-QAM modulation scheme are calculated. The average BEP computation for the general quadrature amplitude modulation can be easily managed if the computation for modulation schemes was understood well With 32-FSK, PAM, DPSK, 16QAM, 32QAM 64QAM and

128-QAM the BEP in AWGN channel, demoted noted by P_b, was obtained as [72]

$$P_b = Q\left(\sqrt{2\gamma}\right) \tag{3.48}$$

Where γ the variable denotes symbol SNR. Note also that symbol SNR was the same with bit SNR in case of modulation scheme. The Gaussian Q function was defined as

$$Q(x) = \frac{1}{2\pi}\int_{x}^{\infty} e^{\frac{-t^2}{2}}\,dt \tag{3.49}$$

In fading channels where γ was corrupted by the random fading channel, (3.3) can be taken as the instantaneous BEP expression and the average BEP, which we denote by Pb, was calculated by integrating it over SNR distribution:

$$\overline{P_b} = \int_{0}^{\infty} p_b\, f_\gamma(\gamma)dy = \int_{0}^{\infty} Q\left(\sqrt{2\gamma}\right) f_\gamma(\gamma)dy \tag{3.50}$$

where $f_\gamma(\gamma)$ was the PDF of the SNR. Various PDF expressions have been computed in the previous chapter for different fading channel models. Before we start analyzing (3.34) for fading channel models, let us first make the equation suitable for integration by substituting $Q\left(\sqrt{2\gamma}\right)$ with an alternative expression [73].

$$Q(x) = \frac{1}{\pi}\int_{0}^{\frac{\pi}{2}} \exp\left(\frac{-x^2}{2\sin^2\theta}\right)d\theta \qquad \text{for } x \geq 0 \tag{3.51}$$

After using this alternating expression and MGF definition equation (3.34) can be reduced into form

$$\overline{P_b} = \frac{1}{\pi}\int_{0}^{\frac{\pi}{2}} M_\gamma\left(\frac{-1}{\sin^2\theta}\right)d\theta \tag{3.52}$$

i. Rayleigh Fading Channel

Substituting MGF expression (3.8) of Rayleigh fading channel, (3.36) becomes

$$\overline{P`_b} = \frac{1}{\pi}\int_{0}^{\frac{\pi}{2}} \frac{1}{1+\frac{\bar{\gamma}}{\sin^2\theta}}d\theta \tag{3.53}$$

This integration is further modified as follows:

$$\overline{P_b} = \frac{1}{\pi}\int_0^{\frac{\pi}{2}} \frac{1}{1+\frac{\overline{\gamma}}{\sin^2\theta}}\,d\theta = \frac{1}{2} - \frac{\overline{\gamma}}{\pi}\int_0^{\frac{\pi}{2}} \frac{1}{\overline{\gamma}+\sin^2\theta}\,d\theta \tag{3.54}$$

Here we can apply the indefinite integral

$$\int \frac{dx}{a+b\sin^2 x} = \frac{1}{\sqrt{a(a+b)}}\arctan\left(\sqrt{\frac{a+b}{a}}\tan x\right) \qquad for \quad a>0 \tag{3.55}$$

By combining (3.51) and (3.52), we obtain [74]

$$\overline{P_b} = \frac{1}{2}\left(1-\left(\sqrt{\frac{\overline{\gamma}}{\overline{\gamma}+1}}\right)\right) \tag{3.56}$$

ii. Rician Fading Channel

Let us substitute the Rician fading channel MGF expression (3.12) into (3.42), then we get [75]

$$\overline{P_b} = \frac{1}{2}\int_0^{\frac{\pi}{2}} \frac{(K+1)\sin^2\theta}{(K+1)\sin^2\theta+\overline{\gamma}}\exp\left(\frac{-K\overline{\gamma}}{(K+1)\sin^2\theta+\overline{\gamma}}\right)d\theta \tag{3.57}$$

iii. Nakagami Fading Channel

MGF for Nakagami fading channel is given in equation (3.18). When it is combined with (3.18), we obtain

$$P_b = \frac{1}{\pi}\int_0^{\frac{\pi}{2}} \left(\frac{\sin^2\theta}{\sin^2\theta+1}\right)^m d\theta \tag{3.58}$$

Where $c = \frac{\overline{\gamma}}{m}$

3.3. Average Capacity

Channel capacity defines the maximum data rate that can be sent over the channel with asymptotically small error probability. It represents an optimistic upper bound for practical

communication schemes; therefore, it serves as a standard against which to compare the spectral efficiency of all practical transmission schemes. Based on available information at the transmitter and receiver about the time-varying channel and type of adaptive transmission policy used by the transmitter, various definitions are used to calculate capacity of at fading channel [76]. We follow the definition of capacity in case the transmitter cannot adapt its transmission strategy relative to the channel fade information which was available at only the receiver. Given that BW was the bandwidth of the system, Ergodic capacity was obtained by averaging the capacity of an AWGN channel. Therefore, AWGN channel capacity, denoted by C^{AWGN}, and average capacity, denoted by C, are formulated, respectively as follows:

$$C^{AWGN} = BW.\log_2(1+\gamma) \tag{3.59}$$

$$C = \int_0^{\infty} BW.\log_2(1+\gamma) f_{\gamma}(\gamma) d\gamma \tag{3.60}$$

With the help of the logarithmic identity $\log_a^b = \frac{\log_c^b}{\log_c^a}$ equation (3.73) was simplified into form

$$C = \frac{BW}{\ln(2)} \int_0^{\infty} \ln(1+\gamma) f_{\gamma}(\gamma) d\gamma \tag{3.61}$$

Rayleigh Fading Channel

Substituting PDF expression of Rayleigh fading channel given in (3.17) into (3.74), we find that [77]

$$C = BW \int_0^{\infty} \ln(1+\gamma) \exp\left(\frac{-\gamma}{\bar{\gamma}}\right) d\gamma \tag{3.62}$$

Performing change of integration variable to $y = 1+\gamma$, Equation (3.75) is reduced into

$$C = \frac{BW}{\ln(2)\bar{\gamma}} \exp\left(\frac{1}{\gamma}\right) \int_1^{\infty} \ln(y) \exp\left(\frac{-y}{\bar{\gamma}}\right) dy \tag{3.63}$$

$$C = \int_1^{\infty} e^{-\mu x} \ln(x) dx = -\frac{1}{\mu} Ei(-\mu) \tag{3.64}$$

$$C = \frac{BW}{\ln(2)} \exp\left(\frac{1}{\bar{\gamma}}\right) Ei\left(\frac{1}{\bar{\gamma}}\right) \tag{3.65}$$

Where Ei (.) was the exponential integral function,

$$\mathrm{Ei}(x) = -\int_{-x}^{\infty} \frac{e^{-t}}{t} dt = \int_{-\infty}^{x} \frac{e^{t}}{t} dt \tag{3.66}$$

Rician Fading Channel

Making use of the PDF of from (3.11), (3.62) was simplified for Rician fading channel into [78]

$$C = \frac{BW}{ln(2)} \int_0^{\infty} ln(1+\gamma) \frac{(1+K)e^{-K}}{\overline{\gamma}} exp\left(-\frac{(1+K)\gamma}{\overline{\gamma}}\right) . I_o\left(\frac{\sqrt{4K(1+K)\gamma}}{\overline{\gamma}}\right) d\gamma \tag{3.67}$$

$$C = \frac{BW}{\ln(2)} \frac{(1+K)e^{-K}}{\overline{\gamma}} \sum_{n=0}^{\infty} \frac{1}{(n!)^2} \left[\frac{K(1+K)}{\overline{\gamma}}\right]^n x\, G_{3,2}^{3,1}\left[\frac{K+1}{\overline{\gamma}}\middle|_{0\,,-1-n}^{-1-n} \quad {}_{-1-n}^{-n}\right]$$

Nakagami Fading Channel

Using the PDF expression in (3.23), Equation (3.45) was reduced into form [79]

$$\mathrm{C} = \frac{\mathrm{BWm^m}}{\ln(2)\overline{\gamma}^{\mathrm{m}}\mathrm{r(m)}} \int_0^{\infty} \gamma^{\mathrm{m}-1} \ln(1+\gamma) \mathrm{e}^{\frac{-\mathrm{m}\gamma}{\overline{\gamma}}} \mathrm{d}\gamma \tag{3.68}$$

For integer m, the integration in (3.81) is solved. Using the result from there and the identity r (m) = r (m-1)! For an integer m, (3.81) becomes

$$C = \frac{BW}{ln(2)} e^{\frac{m}{\overline{\gamma}}} \sum_{k=1}^{m} \left(\frac{m}{\overline{\gamma}}\right)^{m-k} \mathrm{r}\left(-m+k, \frac{m}{\overline{\gamma}}\right), \tag{3.69}$$

Where r(.,.)is the incomplete gamma function which is defined as?

$$\mathrm{r}(\alpha, x) = \int_x^{\infty} e^{-t}\, t^{\alpha-1} dt \tag{3.70}$$

Making change of summation parameter such that l = m-k,

$$C = \frac{BW}{ln(2)} e^{\frac{m}{\overline{\gamma}}} \sum_{l=0}^{m-1} \left(\frac{m}{\overline{\gamma}}\right)^{l} \mathrm{r}\left(-l, \frac{m}{\overline{\gamma}}\right), \tag{3.71}$$

Furthermore, an equation has formulated a closed form expression for C when m is arbitrary. The expression is presented as follows:

$$C = \frac{BW}{ln(2)} \frac{1}{\mathrm{r}(m)} \left(\frac{m}{\overline{\gamma}}\right)^{m} G_{2,3}^{3,1}\left[\frac{m}{\overline{\gamma}}\middle|_{0,}^{-m,} \quad {}_{-m}^{1-m}\right] \tag{3.72}$$

Chapter Four: Result and Discussion

4.1. Rician and Nakagami PDF simulation result

It can be observed that for K = 0 the channel exhibits Rayleigh fading, and when K = ∞ the channel does not exhibit any fading at all. The pdf of the envelope $P_r(r)$ was shown in Fig 4.1 for various values of K. From the plots it can be observed that for K = 0 the pdf was a Rayleigh distribution and for K>>1 the Pdf becomes approximately Gaussian with a mean square value (power)s . In Fig. 4.1 the mean square values of the pdf have been normalized to one. Similar to the Rayleigh distribution, when the time delays $\tau_k(t)$ are on the order of and larger, the random phase terms are essentially uniformly distributed over the interval [0,2π), resulting in a uniformly distributed random phase for the scattered components.

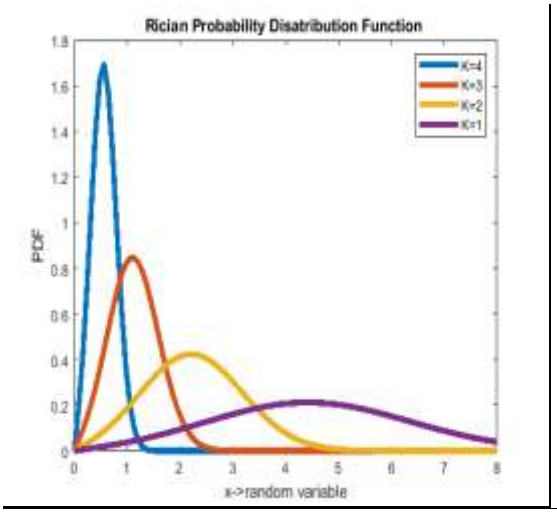

Figure 4.1 Rician probability Distribution function

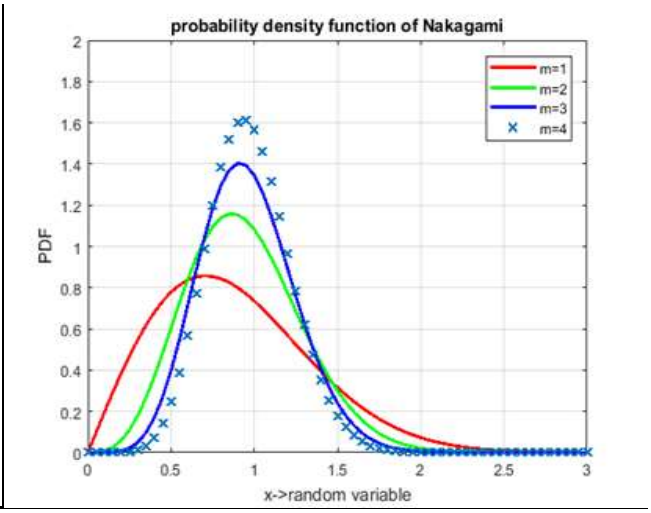

Figure 4.2 Nakagami – m fading Probability distribution function

An example time series of the Rician fading samples was shown in Fig. 4.1 for K= 4 db. As expected, the presence of the specular or the LOS component reduces the number of deep fades when compared to the Rayleigh distribution time series in Fig. 4.3. For the simulations used to generate Fig. 4.1 we used N =100,000 samples with the mean square value for each case set equal to one. When m= 1, the Nakagami distribution is the Rayleigh distribution, when m=1/2 it was a one-sided Gaussian distribution, and when m→∞the distribution becomes an impulse (no

fading) Two useful relations in our case are those relating the Nakagami-m shape factor m and the Rician k factor and σ^2 (the power of the scattered waves). Note that the above relations between m and k and not exact but approximations. Since the Rice distribution contains a Bessel function while the Nakagami distribution does not, the Nakagami distribution often leads to suitable closed-form analytical expressions that are otherwise unattainable. Since the Rice distribution contains a Bessel function while the Nakagami distribution does not, the Nakagami distribution often leads to convenient closed-form analytical expressions those are otherwise unattainable Note that the parameters discussed here are for a non-static channel. If a channel is not changing with time, it does not fade and instead remains at some particular level. Separate instances of the channel in this case will be uncorrelated with one another, owing to the assumption that each of the scattered components fades independently. Once relative motion is introduced between any of the transmitter, receiver, and scatters, the fading becomes correlated and varying in time.

4.2. Simulation result of PDF Rayleigh and four fading channel at once

Since it is based on a well-studied distribution with special properties, the Rayleigh distribution lends itself to analysis, and the key features that affect the performance of a wireless network have analytic expressions

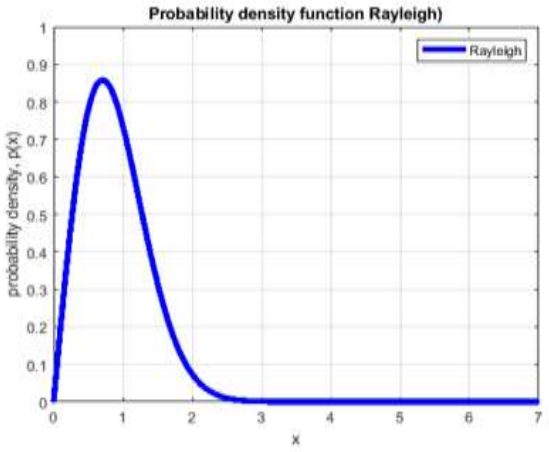

Figure 4.3 Probability Distribution Function of Rayleigh Channel Fading

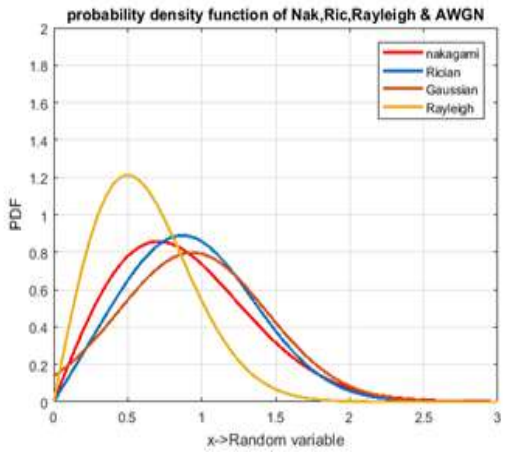

Figure 4.4 Probability Distribution Function of four Channel Fading

Note that the parameters discussed here are for a non-static channel. If a channel is not changing with time, it does not fade and instead remains at some particular level. Separate instances of the channel in this case will be uncorrelated with one another, owing to the assumption that each of the scattered components fades independently. Once relative motion is introduced between any of the transmitter, receiver, and scatters, the fading becomes correlated and varying in time. When we compare the pdf of Rician, Rayleigh, AWGN and Nakagami-m in the Rician K-factor K=0 the Rician become Rayleigh and also if K-factor = ∞ the Rician become AWGN that means no fading. From this result the Rayleigh PDF high from other channels fading.

4.3. Comparison of probability distribution

4.3.1. Rayleigh vs. Nakagami-m fading channel

In dissimilarity to Rayleigh distribution, which has a single parameter to match the fading channel statistically, and Nakagami-m is a two parameter model involving the parameter m. As a consequence, this distribution provides more flexibility and accuracy when matching the observant signal statistically. In a special case m=1, Rayleigh fading are recovered with an exponentially distributed instantaneous power and form>1 the fluctuations of the signal strength was reduced when comparing to Rayleigh fading.

4.3.2. Rayleigh vs. Rician fading channel

Rayleigh distribution has a single parameter and Rician distribution was double. Rayleigh model excludes the effect of a dominant line-of-sight component which is included in Rician model to make it better describes a microcellular propagation process. When Rician factor K goes to minus infinity, Rician distribution will degenerate as Rayleigh distribution.

4.3.3. Rician vs. Nakagami-m fading channel

Rician and Nakagami-m model behave approximately the same near their mean value. Rician and Nakagami-m models have a fundamentally different pdf for deep fades. When modeling a Rician fading signal by Nakagami-m distributed amplitude, results will be overly optimistic with orders of amplitude discrepancies

4.4. Performance Comparison channel model

4.4.1. Simulation Parameters [51-52]

Parameters	Values
Number of FFT points	512
Channel fading	AWGN, Rayleigh, Rician, Nakagami-m
Sub band size	20
Number of sub bands	10
Sub band offset	156
Filter length	43
Side lobe attenuation	40
Bits per subcarrier	2,4,6,8
SNR(dB)	0-40
Modulation schemes	32-FSK, PAM, DPSK,4-QAM, 16-QAM, 32-QAM, 64-QAM and 128-QAM

4.5. AWGN channel fading performance under different modulation schemes

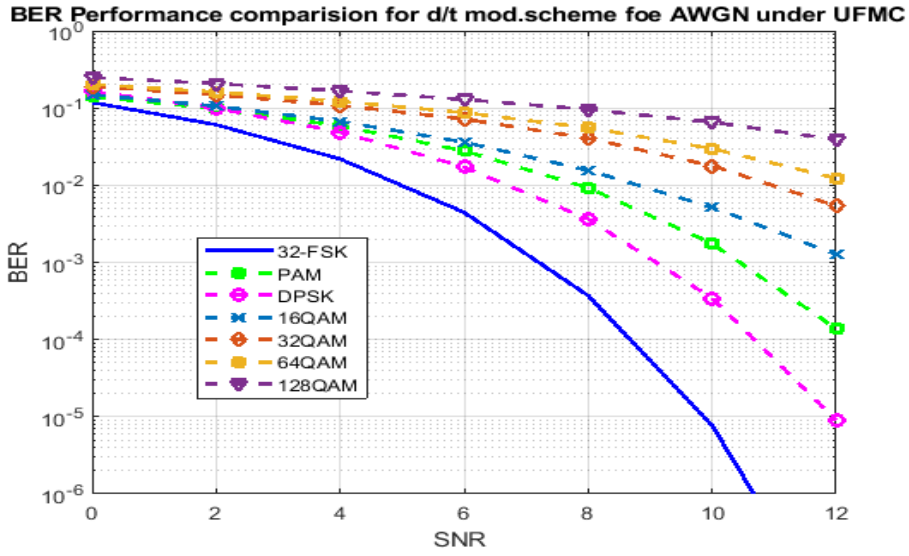

Figure 4.5 BER performance comparison for different modulation schemes for AWGN channel

When the performance comparison of channel model in the figure 4.5 it is clearly seen that if we want to maintain BER vs. SNR the AWGN channel cost least power than other fading channel where Rician, Nakagami-m, and Rayleigh channel have high demands on power. In addition to

this if the BER is increase the SNR will be decrease and also if the BER is decrease the SNR will be increase, as conclude this from shown graph 4.5 AWGN channel fading the better performance. BER performance for various digital modulation schemes like 32-FSK, PAM, PSK, DPSK, OQPSK 16-QAM, 32-QAM, 64-QAM and 128-QAM analyzed for AWGN channel fading FSK better than modulation schemes. Fig.4.5 shows performance analysis of 32-FSK, PAM, DPSK, 16QAM, 32QAM 64QAM and 128-QAM modulation technique over Additive White Gaussian Noise channel using UFMC. In graph as the value of SNR is increases, BER is decreases abruptly in 32-FSK.

Table 4-1 COMPARISON OF BER VS. SNR OVER AWGN

SNR (dB)	BER of AWGN channel fading						
	16-QAM	32-QAM	64QAM	128-QAM	DPSK	PAM	32-FSK
2	0.1453	0.1465	0.1409	0.1498	0.094	0.1209	0.0840
4	0.100	0.1352	0.1349	0.1490	0.0892	0.0942	0.0462
6	0.0987	0.1002	0.1210	0.1480	0.0259	0.054	0.0082
8	0.0923	0.1092	0.1230	0.1430	0.00576	0.0094	0.000567
10	0.0412	0.0923	0.9972	0.1044	0.000456	0.0034	0.000099
12	0.0031	0.0098	0.0192	0.0998	0.0000094	0.0004	0.000000042

4.6. Rayleigh channel fading performance under different modulation schemes

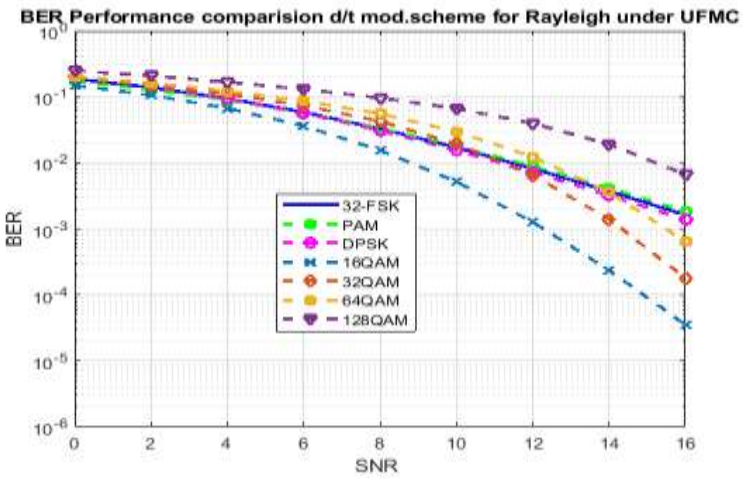

Figure 4.6 BER performance comparison for different modulation schemes for Rayleigh channel fading

Table 4-2 COMPARISON OF BER VS. SNR OVER RAYLEIGH

SNR (dB)	BER of Rayleigh channel fading						
	16-QAM	32-QAM	64QAM	128-QAM	DPSK	PAM	32-FSK
2	0.1231	0.3465	0.3931	0.4234	0.3450	0.3410	0.3430
4	0.0764	0.1923	0.2419	0.4561	0.1810	0.1780	0.1780
6	0.0694	0.0941	0.0981	0.3411	0.0842	0.0842	0.0842
8	0.0341	0.0844	0.0764	0.0991	0.0791	0.0794	0.0794
10	0.00549	0.0434	0.0651	0.00898	0.0382	0.0409	0.0409
12	0.0021	0.00735	0.042	0.0076	0.00824	0.094	0.092

BER performance for various digital modulation schemes like 32-FSK, PAM, DPSK, 16-QAM, 32-QAM, 64-QAM and 128-QAM analyzed for Rayleigh channel fading 16QAM was better than other modulation schemes. Figure 4.6 performance analyses of 32-FSK, PAM, DPSK, 16-QAM, 32-QAM, and 64-QAM and 128-QAM modulation schemes over Rayleigh fading channel. 16-QAM has lower BER than

32-FSK, PAM, DPSK, 32-QAM, 64-QAM and 128-QAM. For example at SNR=4, BER in 16QAM is = 0.0764 where the other modulation schemes are greater than 0.0764is around 0.1923 and above. At SNR=12, 16QAM, BER=0.0021 but other modulation schemes are above BER>0.042.

4.7. Rician channel fading performance under different modulation schemes

BER performance for various digital modulation schemes like 32-FSK, PAM, DPSK, 16-QAM, 32-QAM, 64-QAM and 128-QAM analyzed for Rician channel fading DPSK was better than other modulation schemes the difference between Rayleigh and Rician was in the Rayleigh channel fading PSK was less performance than FSK, but in the Rician channel fading both PSK and FSK approaches to same performance. Figure 4.7 shows BER vs. SNR performance analysis of 32-FSK, PAM, DPSK, 16-QAM, 32-QAM, and 64-QAM and 128-QAM modulation scheme over Rician fading channel. We know that if BER decreases than BER performance will be increases. In graph as the value of SNR is increases, BER is decreases in all nine modulation scheme, that mean for better performance signal to noise ratio must be high i.e. noise must be low for best communication. Here BER performance of, DPSK is better than 32-FSK, PAM,

DPSK, 16-QAM, 32-QAM, 64-QAM and 128-QAM. When you generate the data at SNR 2 dB and 4dB it is equal but as you increase the values of SNR the BER also increase when go to SNR 10dB and 12dB the DPSK increase the performance compare to other modulation schemes.

So when you see from the graph DPSK was better.

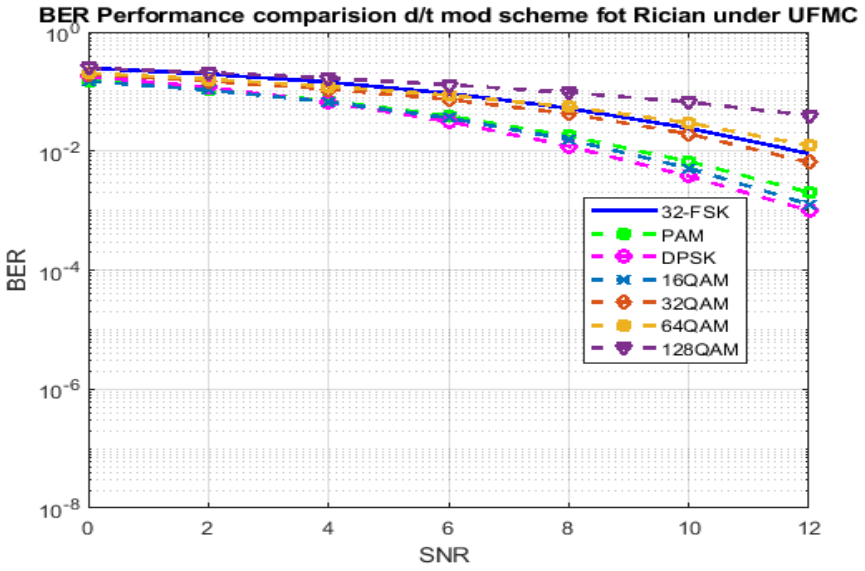

Figure 4.7 BER performance comparison for different modulation schemes for Rician channel fading

Table 4-3 COMPARISON OF BER VS. SNR OVER RICIAN

SNR (dB)	BER of Rician channel fading						
	16-QAM	32-QAM	64QAM	128-QAM	DPSK	PAM	32-FSK
2	0.1201	0.3412	0.3200	0.3451	0.1304	0.1201	0. 3210
4	0.0710	0.1321	0.1450	0.2354	0.0710	0.0710	0.1921
6	0.0656	0.0964	0.0982	0.2194	0.0650	0.0589	0.990
8	0.0450	0.0650	0.0756	0.01	0.0357	0.0492	0.0824
10	0.0568	0.0679	0.0872	0.00721	0.0498	0.0792	0.0724
12	0.0024	0.0072	0.0192	0.00569	0.001	0.0049	0.0098

Table 4-4 BER OF MQAM FOR DIFFERENT VALUES OF K, M (SNR=0-30dB)

Different values of K	**Bit error rate**		
	M=4	**M=8**	**M=16**
K=0dB	0.00019	0.00094	0.0037
K=6dB	0.0000018	0.000011	0.00028
K=12dB	0.00000075	0.0000027	0.000059

Figure 4.8, 4.9 Figure 4.10, shows the bit error rate of MQAM over Rician fading channel with 5G UFMC modulation techniques versus the mean bit SNR. The bit error rate versus the mean values of the bit SNR is shown for various values of the Rician parameter, that is K = 0 dB, 6 dB, 12 dB for the modulation order of M = 4, 8, 16. The Rician distribution follows Rayleigh distribution for K=0. It is clear from the results that for any value of M, as the value of K increases, the BER reduces. As observed that from the figure 8, for fixed value of K, as the value of M decreases, the BER reduces thereby improving the performance of the system. The Rician channel fading depends up on the factor of K. If the value of k-factor increase the Rician fading goes to AWGN and also if the k- factor decrease the Rician fading will be goes to Rayleigh fading so the performance of Rician fading depend on the k-factor, so as we see the graph above if the values of k=∞ The Rician fading is high performance than Rayleigh fading.

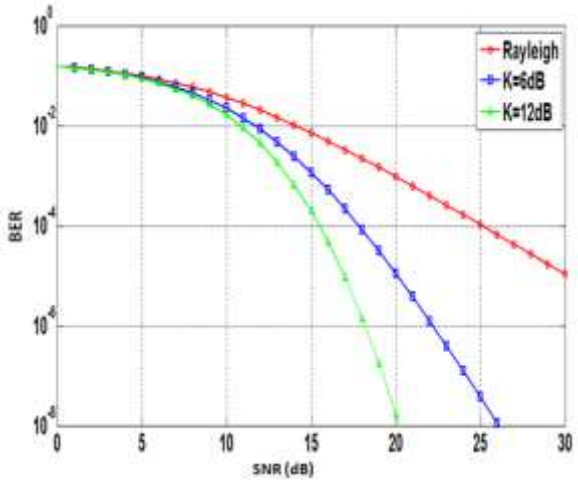

Figure 4.8 BER of MQAM modulation scheme under Rician fading channel for M=8

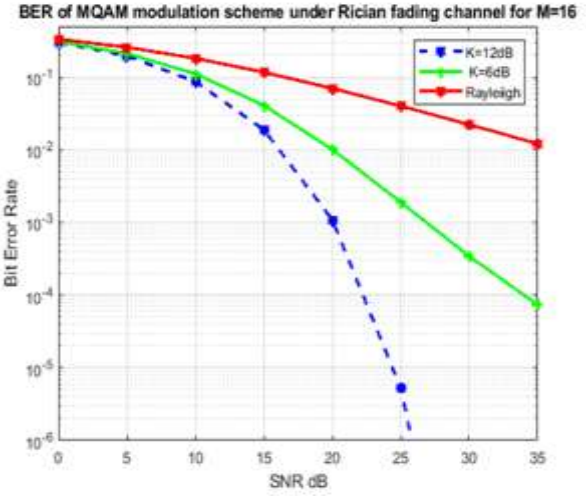

Figure 4.9 BER of MQAM mod. Scheme Under Rician fading channel for M=16.

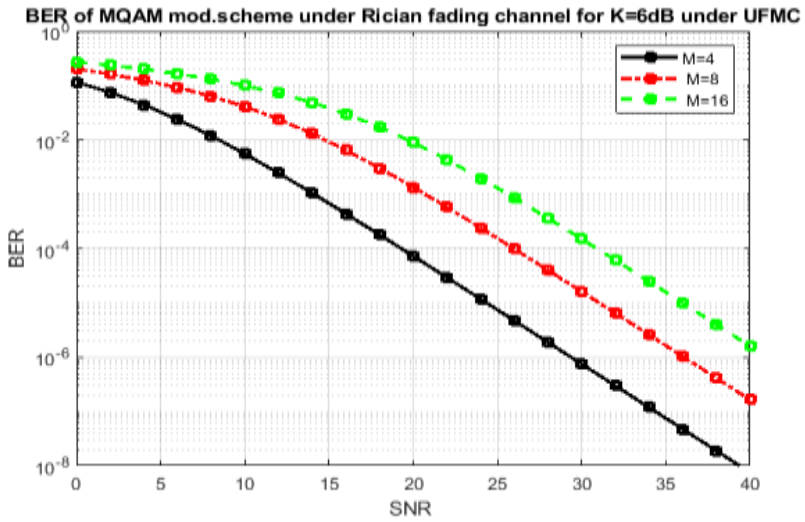

Figure 4.10 BER of MQAM modulation scheme under Rician fading channel for K=6dB.

4.8. Nakagami-m channel fading performance under different modulation schemes

BER performance for various digital modulation schemes like 32-FSK, PAM, DPSK, 16-QAM, 32-QAM, 64-QAM and 128-QAM analyzed for Nakagami-m channel fading DPSK was better than other modulation schemes the difference between Rayleigh and Rician was in the Rayleigh channel fading PSK was less performance than FSK, but in the Rician channel fading both PSK and 32-FSK approaches to same performance.

Table 4-5 COMPARISON OF BER VS. SNR OVER NAKAGAMI-m

SNR (dB)	BER of NAKAGAMI-m channel fading					
	16-QAM	32-QAM	64QAM	128-QAM	DPSK	PAM
2	0.05241	0.0671	0.0842	0.1289	0.0325	0.0475
4	0.04351	0.0625	0.07541	0.0792	0.00865	0.0325
6	0.00985	0.0238	0.0413	0.0675	0.00512	0.00821
8	0.00624	0.00681	0.00752	0.0532	0.00392	0.00521
10	0.00435	0.00496	0.00645	0.0438	0.000852	0.00354
12	0.000876	0.00264	0.00457	0.0349	0.000568	0.000756

Figure 4.10 shows BER vs. SNR performance analysis of 32-FSK, PAM, DPSK, 16-QAM, 32-

QAM, 64-QAM and 128-QAM modulation scheme over Nakagami-m fading channel. We know that if BER decreases than BER performance will be increases. In graph as the value of SNR is increases, BER is decreases in all seven modulation scheme, that mean for better performance signal to noise ratio must be high i.e. noise must be low for best communication. Here BER performance of, DPSK is better than 32-FSK, PAM, DPSK, 16-QAM, 32-QAM, 64-QAM and 128-QAM.

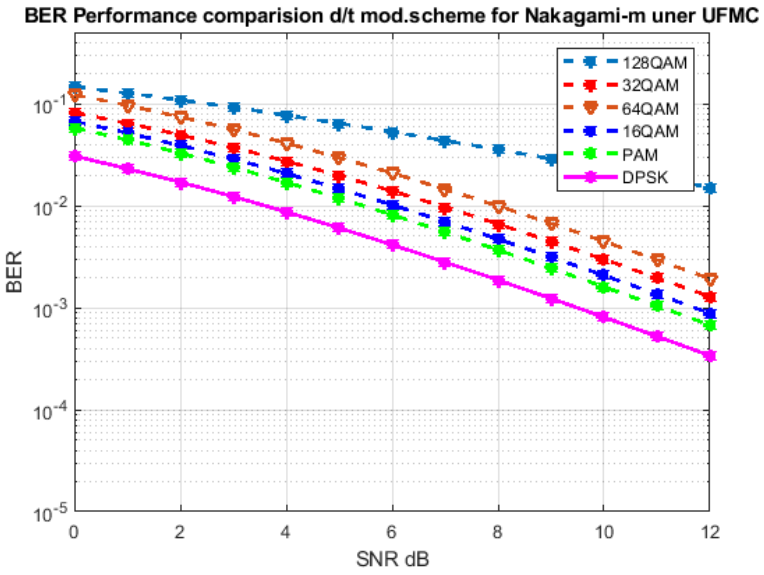

Figure 4.11 BER performance comparison for different modulation schemes for Nakagami-m channel fading

In this section it will be consider how BER depends on average SNR per bit in channel with the Nakagami-m fading during M-ary QAM and other various types of modulation schemes signals transmission. It will also observe the effect of Nakagami parameter m on BER. As shown in figure 4.10 the BER dependence on average SNR in the Nakagami fading m=1 for 4-QAM, 16-QAM, 32-QAM, 64-QAM and 128-QAM. The same dependence but for Nakagami parameter m=2 as shown figure 4.14 when the average SNR in 30dB the values of 4-QAM, 16-QAM, 32-QAM, 64-QAM and 128-QAM is $1x10^{-6}$, $4.12x10^{-5}$, $8.34x10^{-5}$, $7.8x10^{-4}$ and $4.76x10^{-3}$ respectively. With higher order of QAM the performance of BER is worst but the large amount of information was transmitted. As shown in figure 4.11, 4.12 and 4.13 the deeper fading (m=1) the BER curves of the different QAM order are closer than for case of m=2 and m=5.when the impact of fading is lower, the distance between the curves is bigger.

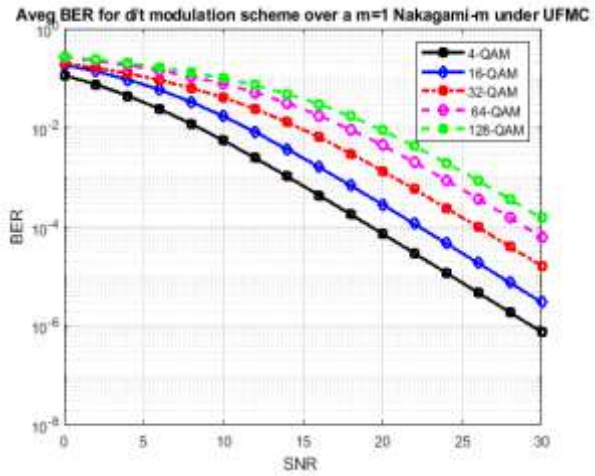

Figure 4.12 BER for different modulation scheme over a m=1 Nakagami-m

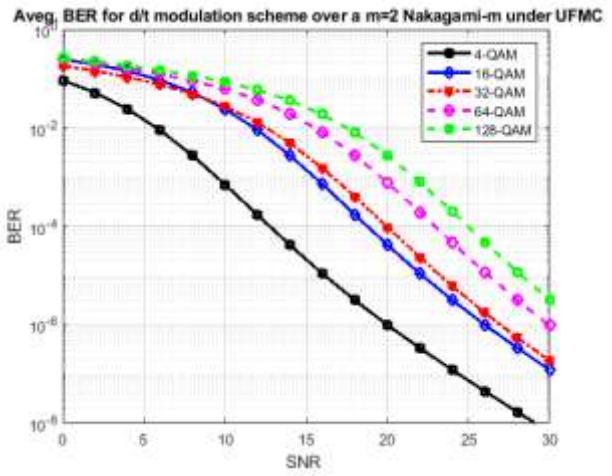

Figure 4.13 Average BER for different modulation scheme over a m=2 Nakagami-m

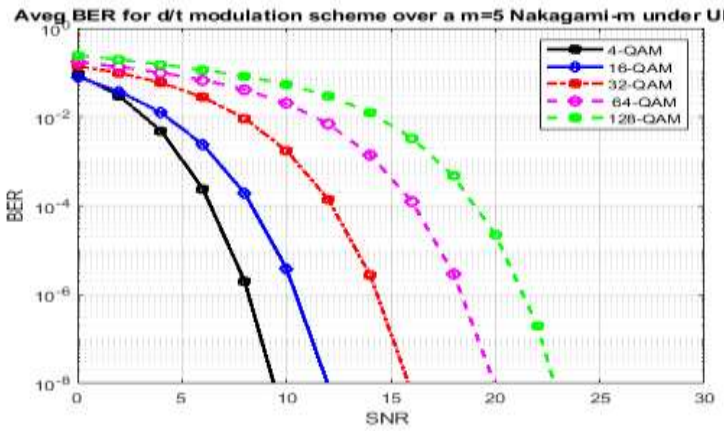

Figure 4.14 Average BER for different modulation scheme over a m=5 Nakagami-m

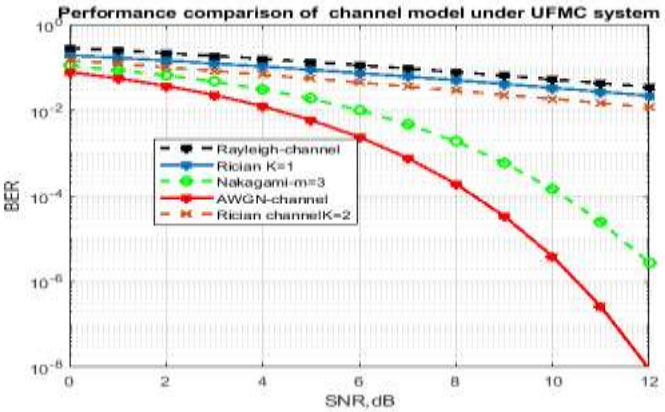

Figure 4.15 Performance comparison of channel model under UFMC

From this comparison AWGN better performance than Nakagami-m, Rayleigh and Rician fading. Next to this Nakagami-m was better performance as we compared to Rayleigh and Rician fading. The performance of Nakagami-m depends on the m value, when we increase the value of m the BER decrease and also the SNR was increase as well. Same that the performance of Rician depends on the value of k factors, as we increase the values of k factor the SNR increase directly and also the BER decrease as well. From this the AWGN fading was better performance than other channel fading.

4.9. Capacity comparison channel fading under UFMC

In this paper the performance comparison channel models for UFMC system as we see in the figure 4.15 the graph simulated in the parameter the capacity verses SNR. As we the SNR increased the capacity of channels also increase directly proportion. Capacity measure is one of the performance measurement parameter of channel models. It also according to simulation result AWGN is high capacity the Nakagami-m, Rayleigh Rician.

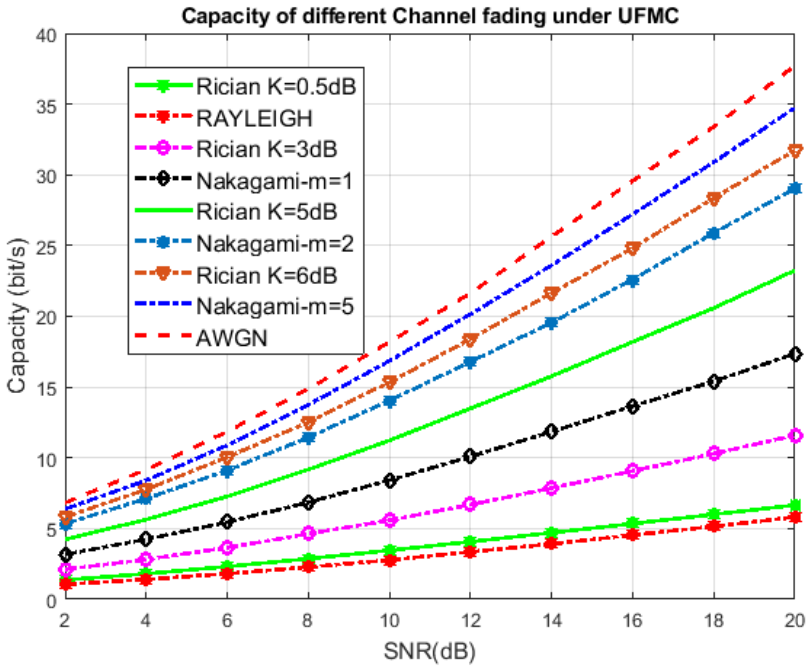

Figure 4.16 Capacity comparison channel fading under UFMC system

Chapter Five: Conclusion and Recommendation

5.1. Conclusion

In this paper, the performance comparison of UFMC system over different channels models with various modulations has been observed. The analysis was based on the study of Bit Error Rate (BER) and Signal to Noise Ratio (SNR). Also explain the design and implementation of UFMC system in terms of operation at transmitter end and receiver end. From the simulation results, the Bit Error Rate (BER) of a wireless communication system was an important figure of merit which used to quantify the integrity of data transmitted through the communication system. By implementing the different modulation techniques, the criterion is comparison of the variation of BER for different SNR. It was observed that the BER was minimum for AWGN and maximum for Nakagami-m, Rayleigh and Rician channel fading.

UFMC was lower peak to average power ratio (PAPR), low out of band (OOB), low latency when compared to other types of 5G modulation techniques. When data is transmitted from transmitter to the receiver through different channels i.e. Nakagami, Rayleigh and Rician fading channels using UFMC, the performance of UFMC depend on the value of filter length, as the value of filter length increase the capacity channel will be increase. When you conclude my thesis by varying the SNR values and filter length to reduce the BER, when you reduce the BER the performance of channel model will be increase in this from AWGN, Rayleigh, Rician and Nakagami-m channel models AWGN was the best channel model. The performance of AWGN channel was the best of all channels as it has the lowest bit error rate (BER) under 32-FSK, PAM, 16-QAM, 32-QAM, 64-QAM and 128-QAM modulation schemes. The amount of noise occurs in the BER of this channel is quite slighter than fading channels. The performance of Rayleigh fading channel is the less performance of all channels as BER of this channel has been much affected by noise under 32-FSK, PAM, 16-QAM, 32-QAM, 64-QAM and 128-QAM modulation schemes. The performance of Rician fading channel less performance than that of AWGN channel and better than that of Rayleigh fading channel. Because Rician fading channel has higher BER than AWGN channel and lower than Rayleigh fading channel. The performance of Rician depends on the value of K factor, as the value of K increase the performance of Rician will be increase and vice versa. When you K values go to 0 the Rician become Rayleigh channel. And also the values of K go to infinity the Rician channel become approach to AWGN. In the

same true the Nakagami-m channel performance depend on the value of m shape factor. As the value of m increase the performance will increase and vice versa. When come to modulation schemes from 32-FSK, PAM, DPSK, 4-QAM, 16-QAM, 32-QAM, 64-QAM and 128-QAM the 4-QAM are the better modulation schemes under UFMC.

My contribution of in this thesis was by comparing the different channel models with in various modulation schemes under UFMC system and identify the preferable for best communication system. By varying the value of K- factor of Rician with in M-ary and m-shape factor of Nakagami-m with in M-ary compare the performance of channel models.

5.2. Recommendation

Further this work can be extended to increase the performance of the UFMC system by using the other channel model types and other parameter measurement such as spectral efficiency, Peak to Average power ratio (PAPR) and using Massive MIMO. Also there is a chance to implement the UFMC system by using different Modulation types.

Reference

[1] P. Naga Rani,Dr. Ch. Santhi Rani," *UFMC: The 5G Modulation Technique*" Volume 2 No 2 May 2018

[2] J. Foschinit, Michael J. Gamt, and Joseph M. Kahn, "*Fading Correlation and Its Effect on the Capacity of Multi-Element Antenna Systems*" Cory Hall, University of California Berkeley, 2017

[3] F .Schaich, Y Chen, "*5G air interface design based on universal filtered (UF-)OFDM*", in 19th International Conference on Digital Signal Processing (DSP).,(2014),

[4] H. Bogucka, *"Advanced Multicarrier Technologies for Future Radio Communication*": 5G and Beyond, John Wiley and Sons, Inc., 2017.

[6] A. Sudhir BabuAssociate Professor, "*Evaluation of BER for AWGN, Rayleigh and Rician Fading Channels under Various Modulation Schemes*" *Volume 26– No.9, July 2011*

[7] P. Bhatnagar, J. Singh, M. Tiwari, "*Performance of MIMO-OFDM system for rayleigh fading channel*" Volume 1 No 3 May 2011

[8] S. Varade**,** K. Kulat "*BER Comparison of Rayleigh Fading, Rician Fading and AWGN Channel using Chaotic Communication based MIMO-OFDMSystem*". Issue-6, January 2012

[9] Dr. K.V Sambasiva Rao, "*Evaluation of BER for AWGN, Rayleigh and Rician Fading Channels under Various Modulation Schemes*", Issue-6, May 2014

[10] Y. Singh1 , Mrs. Anita Chopra, "*Analysis of Rayleigh, Rician and Nakagami-m fading channel using Matlab Simulation*", Volume 3; Issue 4; July-August-2015; Page No. 105-109

[11] V.V. Mani and, S. Kumar Bandari," *Performance analysis of GFDM in various fading channels*" Accepted 1, October-2015

[12] F. Schaich,"*Waveform Contenders for 5g – Suitability for Short Packet and Low Latency Transmissions*", Vehicular Technology Conference, 2014,

[13] Schaich, T. Wild, Yejian Chen. "*Waveform contenders for 5G – suitability for short packet and low latency transmissions*". Vehicular Technology Conference (VTC Spring), 2014 IEEE 79th.

[14] X.Wang, Thorsten Wild, and F.Schaich. "*Filter Optimization for Carrier Frequency- and Timing-Offset in Universal Filtered Multi-Carrier Systems*", Vehicular Technology Conference (VTC Spring), 2015 IEEE 81th.

[15] L. Ahlin, J. Zander, and B. Slimane, "*Principles of Wireless Communica- tions. Overseas*" Press India Private Ltd, 2011.

[16] J. G. Proakis and M. Salehi, "*Digital Communications*", 5th ed. McGraw- Hill, 2008

[17] D.Momen Hasan, S. Sarker, AshrafulAlam, "*Performance Analysis of BPSK and QPSK Under Rayleigh Fading Channel*" Vol.2, No.1, Juny.2014

[18] A. Goldsmith, Wireless communications. Cambridge University Press, 2005.

[19] V,Panwar,S.Kumar,"*Bit Error Rate (BER) Analysis of Rayleigh Fading Channels in Mobile Communication*," IJMER.Vol.2, No.3, June.2012

[20] M. Nakagami, "*A general formula of intensity distribution of rapid* fading," in Statistical Methods in Radio Wave Propagation.

[21] T. S. Rappaport, "*Wireless Communications, Principles and Practice*," Prentice Hall, New Jersey, 2012.

[22] Da-shan Shiu, G.J. Foschinit, Michael J. Gamt, and Joseph M. Kahn, "*Fading Correlation and Its Effect on the Capacity of Multi-Element Antenna Systems*" Cory Hall, University of California Berkeley, 2017

[23] M. Abramowitz and I. A. Stegun, "*Handbook of Mathematical Functions with Formulas, Graphs, and Mathematical Tables*, ninth dover printing, tenth gpo printing ed. New York: Dover, 2010.

[24] K. Kim and G. Shevlyakov, "*IEEE Signal Processing Magazine*, vol. 25, March 2013

[25] R. V. L. Hartley, "*Transmission of Information*," Bell System Technical Journal,vol. 3, pp. 535-564, July 2013.

[26] P. Siohan, C. Siclet, and N. Lacaille, "*Analysis and Design of OFDM / OQAM Systems Based on Filterbank Theory*," IEEE Transactions on Signal Processing, vol. 50, no. 5, pp. 1170-1183, August 2012.

[27] D. Tse, and P. Viswanath, "*Fundamentals of Wireless Communication"*, Cambridge University Press, 2015.

[28] J. G. Proakis, "*Digital Communications*", McGraw-Hill Inc., 4th Edition, 2001.

[29] A. Goldsmith, "*Wireless Communications*", Cambridge University Press, 1st Edition, 2005.

[30] J. G. Proakis, and M. Salehi, *"Digital Communications*", McGraw-Hill Inc., 5thEdition,2007.

[31] E. Biglieri, J. Proakis and S. Shamai,"*Fading channels: Information-theoretic and communications aspects*," IEEE Trans. Inform. Theory,50-th anniversary issue, Oct.2011

[32] . T. S. Rappaport, "*Wireless Communications*", Chs. 3 and 4, Upper Saddle River, NJ: Prentice Hall, 1996

[33] Andrea goldsmith "wireless communications".

[34] B. Sklar, "*Digital Communications: Fundamentals and Applications",* Prentice Hall, 2011.

[35] P. M. Shankar, "*Fading and Shadowing in Wireless System*"s, Springer, 2011

[36] A. Sudhir Babu,, Dr. K.V Sambasiva Rao," *Evaluation of BER for AWGN, Rayleigh and Rician Fading Channels under Various Modulation Schemes",* Volume 26 , July 2011

[37] Wan Fariza Binti Paizi Fauzi , "*Ber Performance Study Of Psk-Based Digital Modulation Schemes In Multipath Fading Environment*", June 2006.

[38] M. Patzold, "*Mobile Fading Channels*". West Sussex, England: John Wiley & Sons, 2002" IEEE Signal Processing Magazine, vol. 25 March 2008.

[40] J. Young, W.R., "*Comparison of Mobile Radio Transmission at 150, 450, 900, and 3700 mc*," Transactions of the IRE Professional Group on Vehicular Communications, vol. 3, no. 1, pp.71{84, Jun 1953.

[41] H. Nylund, *"Characteristics of Small-area Signal Fading on Mobile Circuits in the 150 MHz Band,"* IEEE Transactions on Vehicular Technology, vol. 17, no. 1, Oct -1968.

[42] S. O. Rice, "*Statistical Properties of a Sine Wave Plus Random Noise*," Bell System Tech. J., vol. 27, 2014

[43] J. D. Parsons, "*Mobile Radio Propagation Channel*", 2nd ed. West Sussex, England: John Wiley & Sons, 2010

[44] L.Rubio, J. Reig, Narcís Cardona, "*Evaluation of Nakagami fading behavior based on measurements in urban scenarios*" Communications Department, Technical University of Valencia, Int. J. Electron. Communication.

[45] H. Suzuki, "*A Statistical Model for Urban Radio Propagation*," IEEE Transactions on Communications, vol. 25, no. 7, Jul 2017.

[46] S. Nadarajah and S. Kotz, "*On The Weibull MGF*," IEEE Transactions on Communications, vol. 55, no. 7, July 2007.

[47] J. Cheng, C. Tellambura, and N. Beaulieu, "*Performance of digital linear modulations on Weibull slow-fading channels,"* IEEE Transactions on Communications, , Aug. 2004.

[48] M. De Courville, and P. Duhamel *"Performance analysis of digital modulations on Weibull fading channels,"* Vehicular Technology Conference, 2013. VTC 2003-Fall. 2003 IEEE 58th, Oct. 2013.

[49] Y.-D. Yao and A. Sheikh, "*Outage probability analysis for microcell mobile radio systems with co-channel interferers in Rician/Rayleigh fading environment*," vol. 55, no. 5, August 2008

[50] B. Muquet, Z. Wang, G. B. Giannakis, , "*Cyclic prefixing or zero padding for wireless multicarrier transmissions*" *Communications,IEEE Transactions on*, vol. 50, no. 12, pp. 2136–2148, 2012.

[51] X.Mestre, M.Payaró, Michael Färber3 and Kilian Roth*, "The 5G candidate waveform race: a Comparison of complexity and performance"* on 19 Septamber 2016.

[52] Jun Li, Amitava Bose, and Yiqiang Q. Zhao, "*Rayleigh Flat Fa-+999,ding Channels' Capacity*" on 10 July 2012.

[53] W.Thorste, "*Waveform Contenders for 5G - Suitability for Short Packet and Low Latency Transmissions,* on 27 April 2016.

[54] F. Schaich and T. Wild, "Relaxed synchronization support of universal filtered multi-carrier including autonomous timing advance," in International Symposium on Wireless Communications Systems (ISWCS), 2014.

[55] A. Farhang, N. Marchetti, F. Figueiredo, and J. P. Miranda, "*Massive MIMO and waveform design for 5th generation wirelesscommunication systems,"* in International Conference on 5G for Ubiquitous Connectivity (5GU), 2014,

[56] D. S. Sesia, M. M. Baker, and M. I. Toufik, LTE: *"The UMTS Long Term Evolution: from Theory to Practice"*, 2nd ed. Wiley-Blackwell, 2011.

[57] N. Kim, Y. Lee, and H. Park, *"Performance analysis of MIMO system with linear MMSE receiver*," IEEE Transactions on Wireless Communications, vol. 7, no. 11, pp. 4474–4478, 2008.

[58] D. Chen, X.-G. Xia, T. Jiang, and X. Gao, *"Properties and power spectral densities of CP based OQAM-OFDM systems*," IEEE Transactions on Signal Processing, vol. 63, no. 14, pp. 3561–3575, 2015.

[59] X. Wang, T. Wild, F. Schaich, and A. Fonseca dos Santos, "*Universal filtered multi-carrier with leakage-based filter optimization,*" in European Wireless Conference, 2014,

[60] J. M. Steels, The Cauchy-Schwarz Master Class*: "An Introduction to the Art of Mathematical Inequalities"*. Cambridge University Press, 2004.

[61] D. Chen, X.-G. Xia, T. Jiang, and X. Gao, "*Properties and power spectral densities of CPbased OQAM-OFDM systems,"*IEEE Transactions on Signal Processing, vol.63 2015.

[62] B. Muquet, Z. Wang, G. B. Giannakis, M. De Courville, and P. Duhamel, "*Cyclic prefixing or zero padding for wireless multicarrier transmissions*" Communications, IEEE Transactions on, vol. 50, no. 12, pp. 2136–2148, 2002.

[63] N. Kim, Y. Lee, and H. Park, "*Performance analysis of MIMO system with linear MMSE receiver*," IEEE Transactions on Wireless Communications, vol. 7, no. 11, pp. 4474–4478, 2008.

[64] A. Papoulis, "*Probability, Random Variables, and Stochastic Processes,"* 3rd Edition, McGrawHill, New

[65] Marvin K. Simon and Mohamed-Slim Alouini. "*Digital Communication over Fading Channels",* John Wiley & Sons, Inc York, 1991.

[66] M. Daoud Yacoub, J. Edson Vargas Bautista, and L.Guerra de Rezende Guedes, "*On Higher Order Statistics of the Nakagami-m Distribution*," IEEE Transactions on Vehicular Technology, vol. 48, No. 3, May 1999

[67] J. G. Proakis, "*Digital Communications*", McGraw-Hill, Singapore, Fourth edition, 2001.

[68] M. K. Simon and M. S. Alouini, "*Digital Communications over Fading Channels*", 2nd edition, New York: A John Wiley & Sons, Inc., New York, 2005.

[69] Mohammad Riaz Ahmed, MD. Rumen Ahmed**, "***Performance Analysis of Different M-ary Modulation Techniques in Fading channels using different diversity*," Journal of Theoretical and Applied Information Technology, 2010 p.p 23-28

[70] He and J. Xei, "*BER Performance of M-QAM and MPSK Nakagami fading channel with STTD,*" IEEE Inter. Sympo. On per. Indoor and mobile Radio communication,

[71] Su, Y. T., Chen, J. Y., "*Cut off rates of multichannel MF Sand DPSK signals in mobile satellite communications,* " IEEE Journal on Selected areas in Communications, 2011

[72] Ahmed J. Jmeel, "*Performance enhancement of wireless communication systems using transmit and receive diversity".* 2010 7th International Multi-Conference on Systems, Signals and Devices," IEEE 2010

[73] P. Gupta "*Quadrature Amplitude Modulation*", digital Modulation Techniques" www.digitalmodulation.net/qam.html

[74] Fumiyaki Adachi, "*error Rate Analysis of Differentially Encoded and detected 16-APSK under Rician fading",* IEEE Transactions on Vehicular Technology, Vol. 45, No. 1, February 1996.

[75] Hemant Dhabhai and Ravindra, "*Analysis of BER in FSK Modulation With AWGN Fading Channel,"* VSRD International Journal of Electrical, Electronics & Communication Engg.

[76] A. Goldsmith and P. Varaiya, "*Capacity of fading channels with channel side information," IEEE Transactions on Information Theory*, vol. 43, 1986{1992, nov 1997.

[77] M.-S. Alouini and A. Goldsmith, "*Capacity of rayleigh fading channels under different adaptive transmission and diversity-combining techniques,"* Vehicular Technology, IEEE Transactions on, vol. 48, Jul 2010

[78] W. Yan and Z. Hongbo, *"Outage probability for microcellular mobile radio systems in Rician fading channels*," in CEEM 2000. Proceedings. Asia-Paci_c Conference on Environmental Electromagnetics, 209,

[79] M.-S. Alouini and A. Goldsmith, "*Capacity of Nakagami multipath fading channels," Vehicular Technology Conference*, IEEE 47th, 2012.

Appendix

Appendix A

$$E[X^k] = \int_{-\infty}^{\infty} x^k \, f_x(x)dx \qquad \mu_x = \qquad E[X^k] = \int_{-\infty}^{\infty} x^k \, f_x(x)dx$$

$$VAR[X] = E[(X - \mu x^2)] = \int_{-\infty}^{\infty} (X - \mu x)^2 \, f_x(x)dx$$

$$M_x(s) = E(e^{sx}) = \int_{-\infty}^{\infty} e^{sx} \, f_x(x)d$$

$$\emptyset_x(w) = E\left[e^{jwx}\right] = \int_{-\infty}^{\infty} e^{jwx} f_x(x)dx$$

Appendix B

$$F_{t,k} = \frac{cos\left(Mcos^{-1}\left(\beta cos\left(\frac{\pi k}{m}\right)\right)\right)}{cos[M\cosh^{-1}(\beta)]}$$

$$k = 0, 1, 2 \ldots \ldots where\ \beta = \cosh\left[\frac{1}{m} h^{-1}(10^{\alpha})\right]$$

In linear format is given by

$$y(k) \sum_{i=1}^{n} x_i(n) * f_i(n)$$

$$\underset{[(N+L-1),1]}{X_k} = \sum_{i=1}^{N} \underset{[(N+L-1),N]}{F_{i,k}} \quad \underset{[N,ni]}{V_{i,k}} \quad \underset{[n,1]}{S_{i,k}}$$

Where N: FFT size L: filter length, ni: complex QAM symbol

$F_{i,k}$: is Toeplitz matrixes compose of filter impulse response

$V_{i,k}$: Is an IDFT matrix according to the respective sub band position

$S_{i,k}$: is the symbol of matrix

When we analysis noise variance in UFMC. The time domain zero means AWGN $w(k)$ with variance ${\sigma_n}^2$ is firstly padded with zeros to perform 2N-point FFT at the receiver. The 2N-point FFT of $w(k)$ can be thus written as

$$W_U(k) = \frac{1}{\sqrt{N}} \sum_{l=1}^{N+L-2} w(l)\, e^{-j2\pi lk/2N} \qquad k = 0,1, \dots \dots \dots 2N-1$$

The variance of $W_U(k)$ is given by

$${\sigma_U}^2(k) = E[W_U(k){W_U}^*(k)]$$

Where (.)* denotes conjugates complex operator insert

$${\sigma_U}^2(k) = \frac{1}{N} E\left[\left(\sum_{l=0}^{N+L-2} w(l)\, e^{-\frac{j2\pi lk}{2N}}\right)\left(\sum_{l=0}^{N+L-2} w^*(l)\, e^{-\frac{j2\pi lk}{2N}}\right)\right]$$

$$= \underbrace{\frac{1}{N} E\left[\sum_{l=0}^{N+L-2} w^*(l) e^{-\frac{j2\pi lk}{2N}}\right]}_{= \frac{N+L-1}{N}{\sigma_n}^2} + \underbrace{\frac{1}{N} E\left[\sum_{m=0, m\neq 1}^{N+L-2} \sum_{l=0}^{N+L-2} w(l) w^*(m) e^{\frac{j2\pi(m-l)k}{2N}}\right]}_{= 0}$$

$${\sigma_U}^2(k) = \frac{N+L-1}{N}{\sigma_n}^2$$

The second term is equal zero since w is a white noise, which satisfies

$$E[w(l)w^*(k)] = \begin{cases} {\sigma_n}^2 & if\ l = k \\ 0 & otherwise \end{cases}$$

The derivation holds for all subcarriers. Thus, the noise in every subcarrier k is a zero mean Gaussian-distributed process with the variance of $\frac{N+L-1}{N}{\sigma_n}^2$. The derivation of covariance noise in the UFMC system the covariance between $W_U(l)$ and $W_U(k)$), i.e. noise process in subcarrier l and k, is defined as

$$C_{W_U(l,k)} = E[(W_U(l) - \mathrm{E}[W_U(l)])(W_U(k) - E[W_U(l)])^*]$$
$$= E[W_U(l){W_U}^*(k)]$$

Since $W_U(l)$ is zeros mean and Gaussian-distributed for all subcarriers.

$$C_{W_U(l,k)} = \frac{1}{N} E\left[\left(\sum_{m=0}^{N+L-2} w(m)\, e^{-j2\pi lm/2N}\right)\left(\sum_{m=0}^{N+L-2} w^*(m)\, e^{-j2\pi mk/2N}\right)\right]$$

$$= \underbrace{\frac{1}{N} E\left[\sum_{m=0}^{N+L-2} w(m)w^*(m)\, e^{j2\pi(k-l)m/2N}\right]} + \underbrace{\frac{1}{N} E \sum_{n=0,n\neq m}^{N+L-2} \sum_{m=0}^{N+L-2} w(m)w^*(m) e^{\frac{j2\pi(mk-ln)}{2N}}}$$

$$= \frac{1}{N} \frac{sin\left(\frac{\pi(k-1)}{2N}\right)(N+L-1)}{sin\left(\frac{\pi(k-1)}{2N}\right)} . e^{j\frac{\pi(k-1)}{2N}(N+L-2)} {\sigma_n}^2 \qquad =0$$

$$= c(l.k){\sigma_n}^2 \qquad if\ l \neq k$$

Where $c(l.k)$is given by

$$c(l.k) = \frac{1}{N} \frac{sin\left(\frac{\pi(k-1)}{2N}\right)(N+L-1)}{sin\left(\frac{\pi(k-1)}{2N}\right)} . e^{j\frac{\pi(k-1)}{2N}(N+L-2)} {\sigma_n}^2$$

Obviously, the covariance only depends on the differences between l and k, hence $\Delta k = k - l$ is introduced. Furthermore, all odd subcarriers are dropped in OFDM. Thus, only the covariance between even subcarriers is of interest. We introduce $l' = 2l$ and $k' = 2k$, such that (3.9) the covariance between subcarriers of interest can be formulated as

$$c(l'.k') = \frac{1}{N} \frac{sin\left(\frac{\pi(k-1)}{2N}\right)(N+L-1)}{sin\left(\frac{\pi(k-1)}{2N}\right)} . e^{j\frac{\pi(k-1)}{2N}(N+L-2)} {\sigma_n}^2$$

Appendix C

Consider an UFMC system that consists of N subcarriers allocated to K users with the transmitter and k-th user channel length being $L_{CH,k}$. Zero padding length at the transmitter (on q in equation (3.9)) is LZP and$N_{os,k}$ point DFT is performed at the receiver of the k-th user. A necessary condition for interference-free one-tap channel/filter equalization at the receiver of the k-th user is:

$L_{ZP} \geq L_{CH,k} - 1\ and$

$N_{os,k} = 2^{\eta k} N\ with\ \eta k \geq \left\lceil \log_2\left(\frac{L_{2,k}}{N}\right)\right\rceil$ [57]

and the signal model for the n-th subcarrier of the k-th user in the m-th subband is

$$z_k(n) = \frac{1}{\rho_m \sqrt{2^{\eta k}}} H_k(n,k) F_m(n) a(n) + v_{os,k}(n)$$

Where

$v_{os,k}(n) = \sum_{l=0}^{L_{2,k}} \frac{1}{\sqrt{N_{os,k}}} e^{-j2\pi nl/N} v_k(l)$ is the noise after DFT and down sampling operations.

$H_k(n,k) = \sum_{l=0}^{L_{CH,k-1}} e^{-j2\pi nl/N} h_k(l,t)$ *and* $F_m(n) = \sum_{l=0}^{L_{F,m-1}} e^{-j2\pi nl/N} f_m(l)$ are the channels and filter response in frequency domain respectively.

From equation (3.6), it is obvious that the subcarriers are decoupled in frequency domain and the standard one-tap channel equalization algorithms such as ZF or MMSE can be applied. Note that $L_{CH,k}$and $L_{F,m}$ could be larger than N. If $L_{CH,k} \leq$ N and $L_{F,m} \leq$ N, then $H_k(n,t)$ and $F_m(n)$are the n-th element of N-point DFT transformation of $h_k(t)$ and f_m, respectively. In any case, we have

$E|H_k(n,t)|^2 = {\rho_{CH,k}}^2$

and

$\sum_{n=0}^{N-1} E|F_m(n)|^2 = N_m \sum_{i=0}^{L_{F,m-1}} |f_m(i)|^2 = N_m$ [59]

Interference-free equalization for channel in the UFMC system if we aim to achieve an interference-free system for all place, the condition is specified as $L_{ZP} \geq L_{CH,max-1}$and $N_{os} = 2^{\eta max} N$ with η max ≥ ⌈log2 (L2, max N) ⌉ $\eta max \geq \left\lceil \log_2 \left(\frac{L_{2,max}}{N} \right) \right\rceil$, where$L_{2,max} = max\left(L_{2,k}\right)$ for k = 0, 1, · · ·, K – 1

Consider an UFMC system and the parameters setting for the k-th user satisfying. The SNR at the n-th subcarrier of user k in subband m can be written as:

$$E\{SNR(n)\} = \frac{1}{{\rho_m}^2 2^{\eta k}} \frac{E|H_k(n,t) F_m(n) a(n)|^2}{E\left|v_{os,k}(n)\right|^2}$$

$$= \frac{N}{L_{2,k}} \cdot \frac{{\rho_{sym}}^2}{\sigma^2} \cdot {\rho_{CH,k}}^2 \cdot \frac{1}{{\rho_m}^2} \cdot |F_m(n)|^2$$

Note that $E|H_k(n,t) F_m(n) a(n)|^2 = {\rho_{CH,k}}^2 {\rho_{sym}}^2 |F_m(n)|^2$ since $E|H_k(n,t)|^2 = {\rho_{CH,k}}^2$ and

$E|a(n)|^2 = {\rho_{sym}}^2$. Noise variance is given by $E\left|v_{os,k}(n)\right|^2 = E\left|\sum_{l=0}^{L_{2,k}} \frac{1}{\sqrt{N_{os,k}}} e^{-j2\pi nl/N} v_k(l)\right|^2$

$$= \frac{1}{\sqrt{N_{os,k}}} E\left|\sum_{l=0}^{L_{2,k}} v_k(l)\right|^2 = L_{2,k}/N_{os,k}\sigma^2$$

Substitute $N_{os,k} = 2^{\eta k}N$ and expression of signal and noise power into $E\{SNR(n)\}$ le to [60].

The SNR at the n-th subcarrier depends on the subband index m and the location of the subcarrier in the subband (i.e., index n), i.e., it is proportional to $\frac{1}{{\rho_m}^2}$ and$|F_m(n)|^2$. The latter in general is fixed but varies along the subcarriers in a particular subband. It clearly shows that the filter response depends on filter length and is frequency selective along subcarriers. It is also noted that the variance is considerably large when the filter length increases. When filter length $L_{F,m} = 1$ leads to an OFDM system with sufficient ZP length. Then $F_m(n)$ is constant along the subcarriers and $L_{2,k} = N + L_{CH,k-1}$ with $L_{CH,k-1}$ being the ZP length. We can easily obtain ${\rho_m}^2 = 1$, then signal model in (7) becomes $z_k(n) = \frac{1}{\rho_m\sqrt{2^{\eta k}}} H_k(n,k)F_m(n)a(n) + v_{os,k}(n)$. consequently, (3.12) represents SNR for interference-free ZP-OFDM system as [61]

Appendix D

In the SNR region average capacity per subcarrier can be approximated as

$C_{mUFMC} \approx \frac{1}{N_m}\sum_{n\in U_m} E(\log_2[SNR(n)])$.

Using the expression in (3.14) we have

$$C_{mUFMC} \approx E\left(\sum_{n\in U_m}(\log_2[\alpha 1/{\rho_m}^2|H_k(i.t)|^2)|F_m(n)|^2 =\right.$$

$$= \frac{1}{N_m} E\left(\log_2\left[({\alpha 1/\rho_m}^2)^{N_m}\prod\nolimits_{n\in U_m}|H_k(n,k)|^2|F_m(n)|^2\right]\right)$$

Since it is assumed that the subband is narrowed enough so that the subcarriers lie in the coherent bandwidth

$C_{mUFMC} = \frac{1}{N_m} E\left(\log_2\left[(\alpha 1/{\rho_m}^2)^{N_m} \prod_{n\in U_m} |H_k(n,k)|^2 |F_m(n)|^2\right]\right)$

Where $i \in U_m$. Using inequality arithmetic and geometric means we have

$\left|\prod_{n\in U_m} |F_m(n)|\right|^2 \leq \left(\frac{1}{N_m}\sum_{n\in U_m} |F_m(n)|^2\right)^{N_m} = \left(\frac{1}{N_m} N_m\right)^{N_m} = 1$

Then $C_{mUFMC} \leq \frac{1}{N_m} E\left(\log_2\left[\left(\alpha 1/{\rho_m}^2 . |H_k(i,t)|^2 \frac{1}{N_m}\right)^{N_m}\right]\right)$

$= E\left(\log_2\left[\frac{\alpha 1}{{\rho_m}^2} . |H_k(i,t)|^2\right]\right)$ When ${\rho_m}^2 \geq 1$

Therefore $C_{mUFMC} = E(\log_2[\alpha . |H_k(i,t)|^2])$

The approximation leads to the relationship $C_{mUFMC} = E(\log_2[\alpha 1/{\rho_m}^2 |H_k(i.t)|^2)$ with $\alpha = \frac{N}{{L_{2,k}\rho_{sym}}^2}/\sigma^2$ only when M=1 that is the bandwidth has one subband only.